Tu-Pos537

ALTERATION OF CONDUCTANCE STATE OF LIGHT DEPENDENT CHANNEL IN LIMULUS VENTRAL PHOTORECEPTOR. J.E. Lisman, Brandeis Univ., Biology Dept., Waltham, MA; E.C. Johnson, Marshall Univ., Physiology Dept., Huntington, WV; J. Bacigalupo and C. Vergara, Univ. of Chile, Biology Dept., Santiago, Chile.

The properties of the light-dependent channel in Limulus ventral photoreceptors have been studied in cell-attached patches. Two sizes of single channel events are seen during illumination. The mean open time of the small events is 1.4 msec., about 50% of that of the larger events. The large and small events have the same reversal potential and a similar dependence of open-state probability on voltage. Evidence that these events are due to different conductance states of the same channel comes from analysis of events showing a direct transition between the 15pS and 40pS levels. Expression of the different conductance states is not random; there are long (~0.5 sec) periods in which there are many sequential large events followed by periods in which there are many sequential small events. At early times during the response to a step of light, the large conductance state is preferentially expressed. These changes in the conductance state are of functional importance for light-adaptation.

Tu-Pos538

EFFECTS OF PHOSPHODIESTERASE (PDE) INHIBITORS AND CALCIUM ON PHOTOTRANSDUCTION OF LIMULUS PHOTORECEPTORS. E.C. Johnson, Dept of Physiology, Marshall U. Sch. of Med. Huntington, WV 25755.

If cGMP is the excitatory messenger of phototransduction, then blocking its breakdown should markedly enhance the light response. I studied the effect of PDE inhibitors on the light response in cells injected with different Ca/BAPTA mixtures to "clamp" the intracellular calcium level at 10^{-8}, 10^{-7}, 10^{-6} or 10^{-5} M. Only cells "clamped" to 10^{-7} M Ca^{++} showed a marked effect of superfusion with IBMX (2 mM) by substantially increasing the duration of the light response and slightly increasing the inward current of the cell. To further understand the role of Ca^{++} in determining the activity of the PDE, I studied the response to cGMP injections in the R-lobe before and after injection with EGTA or BAPTA. In all experiments in which the cGMP injection could adequately be controlled throughout there was a >100% increase in the duration of the response to cGMP injection. These results suggest that Ca^{++} (light adaptation) regulates the PDE activity which controls the turn-off of the light response. Supported by NSF-BNS.

Tu-Pos539

COMPUTER MODELLING OF PATTERN FORMATION ON THE VISUAL CORTEX

J. R. Thomson, Z. Zhang, Wm Cowan†, M. Grant, J. A. Hertz‡ and Martin J. Zuckermann, *Department of Physics, McGill University, Montréal, PQ, Canada,* † *Departments of Computer Science and Psychology, University of Waterloo, Waterloo, ON, Canada,* ‡ *NORDITA, Copenhagen, Denmark*

Changes in the connections of neurons in the visual cortex occuring around the time of birth of a primate result in a pattern of occular dominance stripes on layer IV of the cortex itself in primates with normal visual experience. In the case of monocular deprivation during this period, the stripes are no longer regularly spaced and sometimes have the appearence of broken stripes.

We model stripe formation by an intercortical interaction which can in turn be represented by a two-state statistical mechanical model with a long range anisotropic center-surround interaction. We reason that monocular deprivation can be represented by an effective external force. Numerical simulations using a Metropolis Monte Carlo method on a square lattice in conjunction with the two-state model in the presence of such a force are used to predict the effect of monocular deprivation on the striped patterns. The physiological relevance of the results and the direction of future investigations are discussed. This includes a mathematical description of orientation columns on the visual cortex.

Tu-Pos540

GATING KINETICS OF cGMP-ACTIVATED CHANNEL IN CATFISH CONES. L.W. Haynes and K.-W. Yau. Howard Hughes Medical Institute and Johns Hopkins School of Medicine, Baltimore, MD.

Openings of single cGMP-activated channels were recorded from excised, inside-out patches of catfish cone outer segment membrane, with symmetrical solutions containing 118 mM NaCl and no divalents. The prominent openings at low cGMP had a conductance near 45 pS and an open time $\leq$ 0.5 msec. There was also indication of sub-openings. The conductance of the large openings seemed invariant between -50 mV and +50 mV, compared to a slightly outward-rectifying I-V relation for the macroscopic current at saturating cGMP. We attribute this difference to a slightly higher open probability of the fully-liganded channel at positive voltages, which can also explain the smaller $[cGMP]_{1/2}$ for the dose-response relation at positive voltages. The amplitude distribution of low pass-filtered records at saturating cGMP from one patch containing a single channel can be fitted by a beta-distribution, consistent with the fully-liganded channel switching predominantly between a single closed state and the large open state, with opening and closing rates of ca. 2×10^{4} sec^{-1} and 2×10^{3} sec^{-1} at +30 mV. Thus, the sub-openings most probably arose from a partially-liganded state(s) of the channel.

Tu-Pos541

OPENINGS OF SINGLE ROD cGMP-GATED CHANNELS INDUCED BY cAMP. R.S. Dhallan, L.W. Haynes and K.-W. Yau. Howard Hughes Med. Inst. and Johns Hopkins Sch. of Med., Baltimore, MD.

Tanaka, Eccleston & Furman (Biochem. 28: 2776, 1989) have shown that cAMP can open the cGMP-gated conductance in retinal rods. We report here preliminary observations on this cAMP effect at the single-channel level. Patch-clamp recordings were made from inside-out membrane patches excised from toad or frog rod outer segments, with 118 mM NaCl and no divalent cations on both sides. In the presence of 1 μm cGMP or 30-100 μM cAMP, single-channel activity could be detected, with the prominent openings in both cases showing a conductance of ca. 25 pS and similar open times. The saturated macroscopic current induced by cAMP, however, was only ca. 30% of that induced by cGMP. These findings together suggest that cAMP-liganded channels perhaps have a similar closing rate, but a lower opening rate, compared to cGMP-liganded channels. This difference, nonetheless, should make only a small relative contribution (by perhaps a factor of three) to the large difference in channel-activating ability between the two ligands (roughly 100-fold). Thus, most of the difference in effectiveness between cGMP and cAMP is likely to reside in the binding/unbinding kinetics with the channel.

Tu-Pos542

THE ROLE OF IP_3 IN INVERTEBRATE VISUAL TRANSDUCTION. T.M. Frank and A. Fein, Physiology Dept., Univ. of Connecticut Health Center, Farmington, CT 06032

The role of inositol (1,4,5)-trisphosphate (IP_3) in visual excitation of invertebrate photoreceptors has remained controversial. Although IP_3 is capable of depolarizing Limulus ventral photoreceptors in a manner similar to light, the IP_3 response is inhibited in the presence of calcium chelators, while the light response persists. We have examined the role of IP_3 by studying the effects on the light response of heparin, neomycin and BAPTA, agents which disrupt the IP_3 cascade. All three agents inhibit responses to brief flashes of light as well as the transient component of the response to a step of light, suggesting a direct role for IP_3 in light excitation. Additionally, the three agents decrease the amplitude of the plateau component of the step response at low light intensities, while at high intensities, they increase the plateau amplitude. We suggest that a second light activated process, not involving IP_3 and calcium mediated excitation, is responsible for the production of the plateau component of the step response.

Tu-Pos543

COMPARISON OF THE DECAY TIMES OF METARHODOPSIN II AND THE G_v-ACTIVATING SPECIES OF BLEACHED RHODOPSIN, RHO*

Julia Kibelbek, James M. Beach, and Burton J. Litman, Department of Biochemistry, University of Virginia, School of Medicine, Charlottesville, Virginia 22908.

Evidence bearing on the question of the identity of metarhodopsin II (meta II) as rho*, the G_v activating form of photoactivated rhodopsin, was obtained by direct measurement of the decay lifetimes of meta II and rho*, using the same preparations of hypotonically washed rod disc membranes at 20C, pH8.0. The spectral lifetime of meta II using 9-60% bleach was obtained with a multichannel array spectrophotometer between 380-390nm and corrected for light scattering changes. The decay time constant for meta II absorbance was between 11 and 21 minutes, assuming complete first order decay. Decay of rho* was measured by adding aliquots of bleached rhodopsin, after various post-flash incubation times, to a suspension containing G_v and tritiated GMPPNP, a nonhydrolyzable GTP analog, and measuring the rate of G_v activation as indicated by nucleotide exchange. Plots of initial velocities of rho*-catalyzed nucleotide exchange on G_v versus post-flash time fit an exponential decay similar in time dependence to the range obtained spectrally for meta II. These data show the feasibility of comparing the decay lifetime of meta II, determined spectrally, with that of rho*, obtained using G_v activation assays utilizing much lower bleach levels. (supported by NIH grant EY00548).

Tu-Pos544

LINEAR ROD PHOSPHODIESTERSE KINETICS ARE INVARIANT OVER Gpp(NH)p AND ROD DISK MEMBRANE CONCENTRATIONS.

A. E. Barkdoll III and E. N. Pugh Jr.
Department of Psychology, University of Pennsylvania, Philadelphia, PA 19104

We have studied the kinetics of toad rod disk membrane (RDM) phosphodiesterase (PDE) activated linearly by flashes isomerizing $< 10^{-5.5}$ rhodopsin (Rh) using the pH assay of cGMP hydrolysis, with 10 mM cGMP, 0.02 mM to 5.0 mM GppNHp and [RDM] corresponding to 0.7 uM to 17 uM Rh in the reaction cuvette. Activation is first order (time constant τ_D) and invariant over [GppNHp] and [RDM]. (1) While $V_p = V_{max}$ at 125 uM and 0.4 V_{max} at 20 uM GppNHp ([Rh] = 2.4 uM), τ_D is constant over the same range: at 125 uM GppNHp $\tau_D = 15.9 \pm 1.5$ s (n=6), V_p = 2 uM cGMP/s; at 20 uM GppNHp $\tau_D = 17.2 \pm 2.2$ s (n=2), V_p = 0.8 uM/s. (2) While V_p increases linearly over a 25-fold range of [RDM], τ_D is constant: at [Rh] = 0.7 uM $\tau_D = 17.1 \pm 1.8$ s (n=3), $V_p = 0.23 \pm 0.07$ uM cGMP/s (n=3); at 17 uM Rh $\tau_D = 14.2 \pm 1.3$ s (n=5), $V_p = 6.1 \pm 0.06$ uM/s (n=5). Invariance of τ_D over [GppNHp] is consistent with V_p being determined by reversible activation of G-protein by the nonhydrolyzable GppNHp and weak binding of G_α-GppNHp to PDE, but is inconsistent with determination of V_p by exhaustion of fixed pools of G-protein and PDE. Invariance of τ_D over [RDM] is inconsistent with PDE activation being rate limited by aqueous diffusion of G_α-GppNHp.

Supported by NIH Grant EY-02660.

Tu-Pos545

RECORDING FROM SOLITARY PHOTORECEPTORS AND RECONSTITUTED RHADBOMERIC MEMBRANES OF THE SQUID. E. Nasi and M. Gomez, (Intro. by E. Szuts) Dept. of Physiology, Boston University School of Medicine and Marine Biological Laboratory, Woods Hole.

Isolated photoreceptors were obtained by enzymatic dispersion of the retina of Loligo pealii. Nomarski and S.E.M. micrographs reveal that their fine morphological features are preserved: the distal segment is 200-240 um long, 4-6 um wide, and is covered by short microvilli. The intermediate and inner segments, and the cell body with the initial portion of the axon are clearly discernible. Macroscopic current measurements were performed using suction electrode, whole-cell patch and the perforated-patch recording methods, revealing a light-activated inward current graded with light intensity, that could exceed 1200 pA. Its dynamic range is rather compressed, and threshold to saturation occurs in as little as 1.5 log units of light intensity. Bright flashes give rise to a prolonged inward aftercurrent lasting for tens of seconds. On-cell recording yielded a large incidence of silent patches, but on occasions channel activity could be recorded, specifically activated by photostimulation. Vesicles of purified rhabdomeric membranes prepared from squid retinas were fused with planar lipid bilayers under bi-ionic conditions (Na/K). A fast-flickering conductance was observed, reversibly activated by 8 Br-cGMP. Supported by NIH grant EY07559 and by a research grant from the MBL.

Tu-Pos546

TWO COMPONENTS OF THE PHOTOCURRENT IN VOLTAGE-CLAMPED SOLITARY LIMA PHOTORECEPTORS. Enrico Nasi, Dept. of Physiology, Boston University School of Medicine.

Membrane current was recorded from enzymatically dissociated rhabdomeric photoreceptors from Lima scabra, using the whole-cell clamp technique. Light stimulation from a holding potential of -60 or -50 mV evoked an inward current graded with light intensity, accompanied by an increase in membrane conductance. While with dim flashes the photocurrent decays smoothly, at higher stimulus intensities a distinct "hump" appears. The additional component survives superfusion with TEA (20-50 mM), as well as internal perfusion with Cs. Both treatments are effective in eliminating the outward current through the Ca-activated K channels previously shown to exist in these cells. Reversal potential experiments at low light intensities reveal a null potential around 0 mv, but with brighter lights no single voltage is found at which the photocurrent is eliminated: rather, a bi-phasic response with an inward and an outward component can be seen within a certain voltage range. Such feature is retained if the experiment is conducted in the presence of up to 50 mM TEA. Internal perfusion with Cs exerts a blocking effect on the light-sensitive channels in the outward but not the inward direction. These observations suggest the presence of two light-dependent conductances with different kinetics and sensitivities. Supported by grants NSF BNS-84-19942 and NIH RO1 EY07559.

Tu-Pos547

NULL CURRENT MEASUREMENTS PROVIDE ESTIMATE OF INTRACELLULAR Ca IN ROS. G. Rispoli, A.T. Fineberg and P.B. Detwiler. Univ. of Washington, Dept. of Physiol. & Biophys., Seattle, WA.

The highly cooperative Ca regulation of guanylate cyclase (Koch & Stryer, Nature 364:64, 1988) makes dark current (I_d) a sensitive indicator of internal free Ca ($_F[Ca]_i$). This was used to estimate $_F[Ca]_i$ in darkness in dialyzed whole-cell voltage clamped detached outer segments (DOS) from Gecko rods. Under these conditions DOS $_F[Ca]_i$ depends on: 1. Ca influx through light-regulated channels; 2. Ca efflux via Na:Ca, K exchange; and 3. Ca exchange between DOS cytoplasm and dialysis solution. The first two factors are eliminated by removing external Ca and replacing Na with a cation that can permeate the light-regulated channel but can not operate the exchanger; DOS $_F[Ca]_i$ now depends on the free Ca in the dialysis solution ($_F[Ca]_d$). When Ca influx and efflux are abruptly disabled we expect no change in I_d, "NULL CURRENT", if $_F[Ca]_i = {}_F[Ca]_d$. DOS were dialyzed with 0 cGMP, 5 mM ATP, 1 mM GTP, 0.8 mM BAPTA and enough added Ca to set $_F[Ca]_d$ between 5 nM and 1.6 μM. Switching to a 0 Ca (2 mM EGTA) external solution containing Li or guanidinium in place of Na caused a rapid change in I_d, followed by a slower change which depended on $_F[Ca]_d$. Current remained constant when $_F[Ca]_d$ was ~200 nM but increased and decreased when $_F[Ca]_d$ was < and > than 200 nM respectively, suggesting that internal free Ca in DOS in darkness is ~200 nM.

Tu-Pos548

NUCLEOSIDE TRIPHOSPHATES MODULATE THE LIGHT-REGULATED CHANNEL IN DETACHED ROD OUTER SEGMENTS. G. Rispoli and P.B. Detwiler. Dept. Physiol. & Biophys., Univ. of Washington, Seattle, WA.

To study the effect of nucleoside triphosphates (NT) on Ca permeation through light-regulated (L-R) channels the initial change in dark current (I_d) evoked by a rapid change in external Ca (Ca_o) was measured in whole-cell voltage clamped detached outer segments (DOS) of Gecko rods dialyzed with (5 mM ATP, 1 mM GTP, 0 cGMP) or without NT (0 ATP, 0 GTP, 50 μM cGMP) in an internal solution containing 10 mM BAPTA. In NT-depleted DOS, I_d (compared to the value in 1 mM Ca_o) increased 100% in 0 Ca_o and decreased 25% in 10 mM Ca_o. This is consistent with Ca "block" of a channel with a single cation binding site that is occupied by Ca longer than Na. In NT-dialyzed DOS, I_d increased 50% and 15% in 0 and 10 mM Ca_o respectively, indicating that the channel is in a different state than in the absence of NT. One possibility is that in the presence of NT the channel has two cation binding sites that are close enough for bound ions to interact by repulsion. In any case, our results show that nucleoside triphosphates modulate the interaction between Ca and the light-regulated channel. cGMP may also participate in the modulation. In the presence of NT an increase in cGMP, by 0 Ca_o activation of guanylate cyclase, causes an apparent increase in Ca permeability.

Tu-Pos549

LIGHT-ACTIVATED ROD PHOTOTRANSDUCTION ENZYMES DO NOT DIRECTLY MODULATE cGMP-GATED CHANNEL ACTIVITY.

Eric A. Ertel & P.B. Detwiler. Dept. of Physiology & Biophysics, Univ. of Washington, Seattle, WA 98195, USA

Inside-out patches of outer segment membrane from *Gekko Gekko* rods retain a light-sensitive cGMP-induced conductance when prepared in darkness (E.A. Ertel *et al*, Biophys. J. *55*, 458a (1989)). Using this preparation, we have examined the possibility that the light-sensitive channels can be modulated directly by activated transducin or activated phosphodiesterase (PDE), as it was recently suggested (G.B. Krapivinsky *et al*, FEBS Lett. 247, 435 (1989); N. Bennett *et al*, Proc. natn. Acad. Sci. U.S.A. 86, 3634 (1988)). Our results do not support this notion. First, while exposure of a patch to a flash of light in presence of 100μM cGMP and 50μM GTPγS stimulates the transduction machinery irreversibly, addition of 1mM IBMX restores the initial cGMP-induced conductance fully. Second, in presence of 50μM GTP and 5μM 8Br-cGMP, a cGMP-analog more resistant to PDE hydrolysis, the light-sensitivity of the cGMP-induced current is reduced more than 1000-fold compared to that of the similar size current induced by 50μM GTP and 100μM cGMP. Both results indicate that activated transducin does not close the light-sensitive channel by itself but through PDE activation. Finally, activation of PDE by a bright light, in presence of 50μM GTPγS and absence of cGMP, does not open a conductance in our patches, providing evidence against the notion that activated PDE directly opens the cGMP-gated channel in the absence of cGMP.

Tu-Pos550

DIVALENT CATIONS CURRENTS THROUGH CYCLIC GMP-ACTIVATED CHANNELS FROM RETINAL RODS.

G. Colamartino, A. Menini*, L. Spadavecchia* and V. Torre. Dipartimento di Fisica, Universitá di Genova and * Istituto di Cibernetica e Biofisica, C.N.R., Genova, Italy.

Currents activated by 100 μM cyclic GMP were studied in excised inside-out patches from the outer segment of retinal rods of the tiger salamander. Symmetrical solutions containing 110 mM-NaCl, 2mM EDTA, 10 mM HEPES buffered to pH 7.6 with TMAOH were initially present both in the patch pipette and in the bathing solution.

When 110 mM-NaCl in the bathing solution was replaced by equiosmolar amounts (73.3 mM) of chloride salts of divalent cations a small outward current carried by these cations was observed. At +60 mV the ratio of the current was $Na^+ : Sr^{2+} : Ca^{2+} : Ba^{2+} : Mn^{2+} : Mg^{2+}$= 1:0.02:0.014:0.007:0.004:0.003 (the Na^+ current was about 800 pA).

When 1mM divalent cations were added to 110mM-NaCl in the bathing solution the outward Na^+ current was reduced. The blocking efficacy at +100mV was $Mg^2 > Ba^{2+} \approx Mn^{2+} > Ca^{2+} > Sr^{2+}$. The inward Na^+ current was also blocked, but with a different blocking efficacy that, at -100 mV, was: $Ca^{2+} > Ba^{2+} > Sr^{2+} > Mg^{2+} \approx Mn^{2+}$.

These results suggest that divalent cations are permeant blocking ions of the cyclic GMP-activated channel and their effect on the Na^+ current can be interpreted assuming that these cations bind to two distinct sites, one of which appears to be poorly voltage-dependent.

Tu-Pos551

SPATIAL RESTRICTION OF DESENSITIZATION IN NORMAL AND MUTANT FLY PHOTORECEPTORS.

B. Minke and R. Payne *, Dept. of Neuroscience, The Johns Hopkins Univ. Sch. of Med., Baltimore, MD 21205 and *Dept. of Zoology, Univ. of Maryland, College Park, MD 20742.

The suction electrode method for recording from vertebrate rods was applied to fly ommatidia. Illumination of the ommatidium by a 5 μm slit of light (530nm) positioned within the pipette resulted in a flow of current having a waveform similar to that of the receptor potential and a polarity indicating current-flow into the illuminated region of the photoreceptors. The effectiveness of a 5s flash in causing light-adaptation in areas surrounding the slit was localized, having a half-width of 13±2μm (S.E.;n=5) in normal Musca ommatidia. Similar measurements of the effectiveness of a slit in causing light-induced inactivation of phototransduction in ommatidia of the nss (no steady state) mutant of Lucilia also demonstrated localization, with a half-width of 9±1μm (S.E.;n=4). Neither light adaptation in normal ommatidia nor inactivation in the nss mutation therefore appear to be mediated by membrane potential or by a highly diffusible agent.

(Intro. by S.E. Ostroy)

Tu-Pos552

PROLONGED EXCITATION OF LIMULUS VENTRAL PHOTORECEPTORS FOLLOWING INJECTION OF DL-INOSITOL 1,4,5 TRISPHOSPHOROTHIOATE ($DL\text{-}InsP_3S_3$).

R. Payne* and B.V.L. Potter#, *Dept. of Zoology, University of Maryland, College Park, MD 20742 and #Dept. of Chemistry, The University, Leicester, LE1 7RH , U.K.

The role of metabolism in terminating the actions of inositol trisphosphate ($InsP_3$), was investigated by injecting 1mM $InsP_3$ or 1mM $DL\text{-}InsP_3S_3$, an analogue resistant to metabolism, into the light-sensitive lobes of ventral photoreceptors. Injections of either $InsP_3$ or $DL\text{-}InsP_3S_3$ caused an immediate, transient depolarization (amplitude 30-50mV; duration 1-2s). A period of desensitization followed, lasting several seconds, during which further injections were much less effective. Because injection of $DL\text{-}Ins(1,4,5)P_3S_3$ did not result in a prolonged immediate depolarization, this depolarization may be terminated by desensitization rather than by metabolism of $DL\text{-}Ins(1,4,5)P_3S_3$ or $InsP_3$. However, as the sensitivity of the cell returned following injection of $DL\text{-}Ins(1,4,5)P_3S_3$ a series of bursts of depolarization began. Each burst lasted 1-2s and the bursts often continued for tens of minutes. By contrast, no further bursts of depolarization usually occurred after injection of $InsP_3$, possibly due to metabolism of $InsP_3$.

Tu-Pos553

VISION IN PLANTS: LIGHT-INDUCED ION-CURRENTS IN THE GREEN ALGA *CHLAMYDOMONAS REINHARDTII*.

H. Harz and P. Hegemann, MPI für Biochemie, 8033 Martinsried, FRG;

Behavioural light responses of the unicellular alga *Chlamydomonas* consist of a transient stop, immediately following the onset of illumination, and a subsequent orientation towards or away from the light source. The functional photoreceptor for this process has recently been shown to be a rhodopsin.

To identify ionic components in the signal transduction chain, we have applied extracellular recording techniques. Light-induced currents, appearing between 5 and 100 ms after the flash, have been recorded from cell wall deficient cells. They are graded with flash energy and with the calcium concentration of the medium, and both sign and amplitude depends on the orientation of the cell in the pipette. We conclude that light regulates calcium influx in the eyespot region and a subsequent, delayed calcium uptake at the flagellar roots.

Tu-Pos554

A SECOND LIGHT FLASH OR PROLONGED SUPERIMPOSED STIMULI ACCELERATE THE RECOVERY OF TOTAL cGMP IN TOAD ROS.

Christine Blazynski and Adolph I. Cohen. Depts. of Biochem. and Ophthalmol. Washington Univ. Med. Sch., St. Louis, MO 63110.

By quenching biochemistry in pieces of toad retina by rapid freezing (J Biol Chem 261:14142) factors were studied that influence the recovery of total ROS cGMP levels after light exposure. We had reported that the time of recovery following a brief, subsaturating flash is longer (20 sec) than the time reported for recovery of membrane potential (J Gen Physiol 92:731). We now show for two different intensities that when a subsequent flash of the same intensity and duration is applied at 5 sec after an initial flash, the time course for recovery of total cGMP to the dark level is significantly accelerated. Dim continuous illumination reduces cGMP to a stable level and bright flashes (60 msec duration, 1000 times background) superimposed on dim background do not affect the total cGMP level. However, if the superimposed stimulus is continuous, a graded increase in cGMP levels is detected.

Supported by NIH grants EY02294 & EY00258.

Tu-Pos555

EVIDENCE FOR A Na^+/Ca^{2+} EXCHANGER IN BALANUS PHOTORECEPTOR.

J. Smolley and H. Mack Brown (Spon: J.W. Woodbury). Dept. Physiol., Univ. Utah, Salt Lake City, Utah, USA.

Following illumination of the lateral photoreceptor in Balanus, the cell transiently hyperpolarizes due to an electrogenic Na/K exchange. If Li is substituted for Na_o, this hyperpolarization is not only abolished, but a transient 5-15 mV depolarization (post-illumination depolarization, PID) develops when Na_o is restored. PID decays to the resting potential over several minutes. No membrane conductance change occurs during PID. Li substitution of Na also attenuates the depolarizing receptor potential, especially the steady phase of the response. This effect, which is somewhat variable among cells, depends upon the presence of Ca_o. In most cells the effect is rapidly reversible by restoring Na to the bath. The time course of recovery is similar to that of the ADP. These observations suggest that the PID is produced by an electrogenic Na/Ca exchange mechanism which can be unmasked by Li saline. Li saline produces effects that mimic light adaptation which may be the result of accumulation of intracellular Ca.

(Supported by NIH, #NS-07172)

Tu-Pos556

DIMETHYL SULFOXIDE ELEVATES INTRACELLULAR Ca^{2+} AND POTENTIATES PHOTOCURRENT IN A PHOTORECEPTOR.

H. Mack Brown and Bo Rydqvist. Dept. Physiol., Univ. Utah, Salt Lake City, Utah, USA; Dept. Physiol.II, Karolinska Inst., Stockholm, Sweden.

Illumination increases intracellular Ca^{2+} (Ca_i) in invertebrate photoreceptors and decreases it in vertebrate photoreceptors. The change in Ca_i appears to play no direct role in transducing membrane channel conductance in vertebrate rods; it remains uncertain what role changes in Ca_i play in intracellular signal coupling in invertebrate photoreceptors. We report here that the aprotic dipolar solvent dimethyl sulfoxide (DMSO) produces a sustained increase in Ca_i, and light sensitive receptor current and its kinetics are both augmented in Balanus photoreceptors. Current-voltage relations of the photoreceptor membrane in darkness indicate that DMSO may also partially activate the light-sensitive conductance. The co-occurrence of facilitation and activation with increased Ca_i suggests that although DMSO may activate the light-sensitive conductance via increased Ca_i, its major effect is potentiation of an alternative signaling agent.

Tu-Pos557

OPTICAL MEASUREMENTS OF Na-Ca EXCHANGE CURRENTS IN ISOLATED INTACT BOVINE ROD OUTER SEGMENTS. Paul P.M. Schnetkamp, Department of Medical Biochemistry, University of Calgary, Calgary, AB T2N 4N1, Canada. Introduced by J.M. Renaud.

The outer segments of vertebrate rod photoreceptors (ROS) display rather dynamic Ca^{2+} fluxes; Ca^{2+} efflux is exclusively taken care of by Na-Ca exchange. Na-Ca exchange in isolated intact bovine ROS can turnover internal Ca^{2+} at rates exceeding 0.5 mM total Ca^{2+}/s, but due to their small size (typical for mammalian ROS) the maximal Na-Ca exchange current amounts only to 1-2 pA. Here I have applied an optical probe (Schnetkamp, J. Membrane Biol. 88:249, 1985) to measure Na-Ca exchange currents in bovine ROS with a resolution better than 0.02 pA. Na-Ca exchange current was found to be the dominant electrogenic transport pathway for Na^+ and could be measured as forward Na_o-Ca_i exchange (inward current) or reverse Na_i-Ca_o exchange (outward current). Several properties of Na-Ca exchange current in bovine ROS were measured including its dependence on internal and external Ca^{2+} and its dependence on K^+. Supported by MRC and AHFMR.

Tu-Pos558

CALCIUM FLUX IN ROD OUTER SEGMENT MEMBRANES: NEM POTENTIATES THE EFFECTS OF cGMP.
K. BALAKRISHNAN, J. PADGETT AND R.A. CONE, DEPARTMENT OF BIOPHYSICS, JOHNS HOPKINS UNVERSITY, BALTIMORE,MD 21218.

Vesicles from bovine rod outer segment (ROS) membranes were filled with Arsenazo III to monitor Ca^{++} influx activated by adding cGMP (Caretta & Cavaggioni, 1983). Consistent with reports by these and other authors we find that cGMP activates Ca^{++} influx with a $K_{1/2}$ of about 80 uM and in a cooperative fashion, with a Hill coefficient of about 2.2. In each preparation, addition of 1 mM NEM (N-ethylmaleimide) for 10' potentiated the effects of low concentrations of cGMP by decreasing both $K_{1/2}$ and the Hill coefficient by about 1/3. NEM acts by modulating the response to cGMP, since the addition of NEM alone produced no detectable ion flux. Sulfhydryl reagents significantly increase cation permeability in freshly isolated ROS (Cone, Usselman and Wu, ARVO Abstracts, 1984) and alter the amplitude and sensitivity of the photoresponse of frog rods (Donner, Hemila and Koskelainen, 1987). Our results suggest that SH-reagents act directly on the cGMP activated ion channels in ROS.

Tu-Pos559

LIGHT & DARK ACTIVE PDE IN RETINAL RODS. W. H. Cobbs, Biochemistry & Biophysics, U of P School of Medicine, Philadelphia, PA 19104-6059. Kinetic properties of cGMP phosphodiesterase (PDE) in retinal rods of *Ambystoma tigrinum* were derived from currents using jumps of isobutylmethyl xanthine (IBMX), concentration I. In darkness, the first 200 ms fit an exponential transition between [cGMP] steady-states, with time $T_{1/e}$ $(1+ I/K_i)T_0$, K_i 32 uM, T_0 0.23 s, current proportional to $[cGMP]^2$. For simultaneous onset of IBMX and steady light, the intensity just able to offset the induced current at steady-state rose linearly with I. Combinations of IBMX and light producing the same initial current followed the same subsequent light adaptive recovery, independent of isomerizations. For jumps in a continuous light B, the added light to just suppress the induced current was $(D+B)I/K_i$. For K_i 32 uM, the dark-active PDE D matched that excited by 300 rhodopsin isomerizations s^{-1}. Steps of IBMX-inhibition probed the decay of light-activated PDE. The apparent lifetime of PDE at constant current, with B advanced from darkness to 3 x 10^{+5} isomerizations s^{-1}, held fast at T = 0.7+-.2 s as current fell from 50 to 0 pA. The macroscopic PDE activity of isolated rods is proportional to light and independent of adaptive feedback regulation by membrane current. The dark hydrolytic rate constant of 4.3 s^{-1} greatly exceeds excitation by spontaneous thermal isomerization.

Tu-Pos560

REEVALUATION OF CA^{2+} "FLUX" FROM DISK VESICLES
James J. Devenny and James W. Clack (Intro. by W.H. Miller), Dept Ophthal & Vis Sci, Yale School of Med, New Haven, CT.

Numerous studies investigating the cGMP-gated cation conductance in rod disk membranes (RDMs) have measured release of entrapped Ca^{2+} from RDM vesicles using Arsenazo III. The Ca^{2+} ionophore, A23187, has been used *1)* to determine total entrapped Ca^{2+} and *2)* to empty vesicles of Ca^{2+} prior to treatment with cGMP to test whether the cGMP-induced increase in $[Ca^{2+}]_i$ is sensitive to elimination of transvesicular Ca^{2+} gradient.

We have utilized sonication, osmotic shock, and elevation/reduction of external $[Ca^{2+}]$ as additional tests for sensitivity of cGMP- and A23187-induced $[Ca^{2+}]_i$ increases to changes in the transvesicular Ca^{2+} gradient. We find: *1)* in RDM vesicles 50-70% of the cGMP-induced "flux," as well as 90-100% of the A23187-induced Ca^{2+} "flux," is insensitive to elimination of the Ca^{2+} gradient by sonication or osmotic shock in low Ca^{2+} medium (efficacies confirmed by $[^3H]$-inulin entrapment experiments). *2)* raising $[Ca^{2+}]_i$ to as much as 30 µM has no effect on the amplitude or kinetics of the cGMP- and A23187-induced "flux." *3)* While RDM vesicles (or phosphatidylcholine vesicles) loaded with Ca^{2+} by sonication release substantial amounts of Ca^{2+} when sonicated in low Ca^{2+} medium, RDM vesicles loaded with Ca^{2+} by freeze-thawing or adding cGMP in the presence of high Ca^{2+} do not release Ca^{2+} upon sonication in low-Ca^{2+} medium. *4)* A23187 releases Ca^{2+} from PC vesicles which, although devoid of internal Ca^{2+}, have been incubated in a solution containing 1 mM $CaCl_2$. We conclude that:

1. A23187 disrupts binding of Ca^{2+} to proteins and phospholipids as well as releasing entrapped Ca^{2+}.
2. A large fraction of the cGMP-induced release observed in RDM vesicles is due to release of bound Ca^{2+}; ***this indicates the presence of a cGMP-modulated Ca^{2+}-binding protein in RDM which likely participates in transduction.***

Tu-Pos561

Na^+/Ca^{2+}-EXCHANGE AND ADAPTATION IN *LIMULUS* VENTRAL PHOTORECEPTORS. P.M. O'Day, M.P. Keller, and M. Lonergan. Inst of Neuroscience, Univ. of Oregon, Eugene, OR

Na^+/Ca^{2+}-exchange in photoreceptors is essential for regulating $[Ca^{2+}]_i$ and the transmembrane Ca^{2+}-gradient. It is important because Ca^{2+} plays a variety of key roles in photoreceptor function.

We find that Na^+/Ca^{2+}-exchange contributes to light-adaptation (LA) and dark-adaptation (DA). Desensitization induced by an adapting flash (LA) was Na^+_o-dependent: larger with lower $[Na^+]_o$. Na^+-reduction enhanced LA only at intensities above $4x10^{-6}$ W/cm^2. LA was also Ca^{2+}_o-dependent: greater with higher $[Ca^{2+}]_o$. Recovery of sensitivity (DA) was Na^+_o-dependent: DA was slowed in low-Na^+_o, and the recovery level was diminished in low-Na^+_o. Na^+/Ca^{2+}-exchange may contribute to LA and DA by counteracting normal elevations in $[Ca^{2+}]_i$.

We use measurements of $[Ca^{2+}]_i$ and membrane voltage with an analysis of Na^+/Ca^{2+}-exchange to estimate the exchange charge transfer and the time-dependent changes in $[Na^+]_i$ and $[Ca^{2+}_{total}]_i$. Following Na^+_o-removal, transient outward exchange currents reduced $[Na^+]_i$ to below 1 mM in 20 sec. Na^+_o-restoration induced a maintained inward exchange current and a slow rise in $[Na^+]_i$.

Tu-Pos562

DROSOPHILA MUTANT fused rhabdomeres (fur) AFFECTS RHABDOMERE MORPHOLOGY AND PHOTORECEPTOR FUNCTION. A. Blake, P.M. O'Day, T.R. Venkatesh (Intro. by M. Westerfield) Inst Neuroscience & Inst Mol Biol, U of Oregon, Eugene, OR 97403

Photoreceptor cells of the compound eye of Drosophila have elaborately infoldings of the plasma membrane, called rhabdomeres, which are packed with primary photopigment molecules and comprise the region in which phototransduction occurs. We are examining the development of the rhabdomeres and their role in retinal function. We have characterized a new P-element induced mutation, fur, that causes fusion of the rhabdomeres of neighboring photoreceptor cells and longitudunal compaction of the rhabdomere. fur has been localized to the proximal region of the X chromosome by recombination and deficiency mapping. Mutations at fur produce several distinct physiological abnormalities including a 10-fold decrease in retinal sensitivity to light relative to wild-type and the absence of the characteristic prolonged depolarizing afterpotential. The reduction in sensitivity is wavelength-independent. Complete revertants of fur possess normal structure and function.

Tu-Pos563

LIGHT-DEPENDENT ION CHANNELS IN DISSOCIATED PHOTORECEPTORS OF THE SCALLOP. E. Nasi and M. Gomez, (Intro. by S. Levy), Dept. of Physiology, Boston University School of Medicine and Marine Biological Laboratory, Woods Hole

Retinas dissected from the eye of Pecten were enzymatically dissociated, yielding intact, isolated photoreceptors and clumps of cells. Light responsivity in solitary rhabdomeric cells was assessed by membrane current recording, using the "perforated-patch" technique. On-cell patch-clamp measurements in the rhabdomeric (R) lobe revealed single- and multiple-channel inward currents activated by light stimulation, but not by voltage. The channel openings are brief (1-3 ms), and such flickering occurs with or without divalent cations in the electrode filling solution. The unitary conductance was approximately 47 pS, and the reversal potential was about 60 mV positive of resting potential. Channel gating activity was a direct function of light intensity, while the latency of first opening after a flash was inversely related to it. Similar channels were also observed in patches of the somatic membrane adjacent to the R-lobe, but with a lower incidence, and a more prolonged response latency. A different class of channels, mediating an outward current activated by light, but exhibiting also a pronounced voltage dependence, was observed in clumps of cells. Their behavior is consistent with the properties of the hyperpolarizing cells in the distal retina. Supported by NIH grant R01 EY07559.

Tu-Pos564

DENSITY AND SPATIAL DISTRIBUTION OF cGMP-ACTIVATED CHANNELS IN THE SURFACE MEMBRANE OF RETINAL RODS. J.W. Karpen, D.A. Loney, and D.A. Baylor, Dept. of Neurobiology, Stanford Medical School, Stanford, CA 94305.

The density of cGMP-activated channels was measured in membrane patches excised from 40 outer segments of salamander rods prepared in the light. The number of channels in a patch was obtained from the response to saturating cGMP divided by the single channel current. Patch area was calculated from the membrane capacitance. The channel densities ranged from 0.3 to 605 μm^{-2}. The density distribution was much broader than that expected if channels were randomly arranged and present at constant mean density.

To test whether an ordered spatial distribution could account for the density variations, we recorded local light responses from outer segments of transducing rods with a loose patch electrode. The response amplitudes were similar at all radial and longitudinal positions, ruling out spatial variations on a scale greater than the pipette orifice diameter (2.5 μm). Do the density variations observed in excised patches arise from a mechanism that can control the number of active channels in the rod outer segment surface membrane? (Supported by NIH grants EY01543 and EY02005.)

Tu-Pos565

MORPHOMETRIC ANALYSIS OF MYOCYTIC ULTRASTRUCTURAL CHANGES DURING ANOXIA / REOXYGENATION.

A. M. Freedman, J. H. Kramer, I. T. Mak, M. M. Cassidy, E. N. Albert and W. B. Weglicki. Dept. of Medicine. The George Washington University. Washington D.C. 20037

A quantitative ultrastructural analysis was performed using freshly isolated canine myocytes ($1.5x10^6$/ml) exposed to 30 min anoxia (A:95%N_2/5%CO_2) and up to 45 min reoxygenation (R:95%O_2/5%CO_2). Dramatic ultrastructural changes were observed within the first few minutes of reoxygenation. The subsarcolemmal and intermyofibrillar mitochondria become swollen with loosely packed and disordered cristae and rupture sites on the outer membrane: by 20 min R there was a 30% increase in area ($p<0.05$). This correlated with a 25% shape change ($p<0.005$) from the normal ellipsoidal shape to a more spherical shape. The perinuclear mitochondrial area increased non-significantly by 5-10%. Due to mitochondrial swelling the myofibrils were separated from one another. Damage is also observed in the sarcolemma, with prevalent blebbing and membrane loss. The myofibrils show little overall structural injury; however, the Z-line became wider and more diffuse, a 42% increase by 20 min ($p<0.005$). Injury to the nuclear double membrane was observed with complete separation of sections of inner and outer components. Also, loss of nuclear contents into the cytoplasm is evident. This analysis indicates that the injury process proceeds differentially from the exterior to interior. In particular, the mitochondrial round up prior to swelling and finally outer membrane rupturing.

Tu-Pos566

Automatic quantification of axonal transport in living cells by Nanovid Microscopy

H. Geerts, R. Nuyens, R. Nuydens, F. Cornelissen
Dept. Life Sciences, Janssen Research Foundation, Beerse, Belgium

40 nm colloidal gold is taken up by active endocytosis in neuroblastoma cells. The gold labels a population of vesicles, providing excellent contrast in bright-field video-microscopy and which move along neurites by means of axonal transport.
Time sequences of up to 150 seconds are digitised in real-time from video-tape. The colloidal gold probes are detected automatically in the consecutive images, yielding a set of coordinates over the full observation period. A tracking algorithm is then used to calculate histograms of jumplenghts, velocities and stop times. The depression of axonal transport activity by application of 50μM vanadate in a single neurite is illustrated. In addition, intracellular saltatory motion in the non-neuronal PTK_2 cell is studied. The whole procedure, if carefully designed, makes it possible to analyze up to 3 hrs of video-tape per day.

Tu-Pos567

THE EFFECT ON THE 3-D POINT-SPREAD FUNCTION OF THE LIGHT MICROSCOPE, OF THE DEPTH OF THE POINT SOURCE INTO A LAYER OF MEDIUM WITH A MISMATCHED INDEX OF REFRACTION

Sarah Frisken Gibson and Frederick Lanni
Carnegie Mellon University, Pittsburgh, PA 15213

Immersing a point source into a medium such as water or agarose gel, whose refractive index is close to that of cells but significantly different from that of the coverglass, causes severe distortion of the 3-D point-spread function. This distortion is third and higher order spherical aberration which occurs because the optical path lengths of rays that travel through several layers of media with different refractive indices vary in a non-quadratic way with the distance of the ray from the optical axis. The amount of distortion increases dramatically with the depth of the point source into the mismatched medium. Even at depths of only 4 to 10 μm, we have found that this distortion is much more severe than that observed when the refractive index of the immersion oil varies between 1.505 and 1.525.

This poster will present and analyze the distortion in measured 3-D point-spread functions of a light microscope using a high magnification, oil immersion objective lens, as a function of both the depth of the point source into a mismatched medium and the refractive index of the immersion oil. As well, it will present an explanation of these aberrations based on geometric and physical optics. Supported by NIH GM-34639 and Carl Zeiss Inc.

Tu-Pos568

LATENCY IN THE $[Ca^{2+}]_i$ RESPONSE TO IGE RECEPTOR CROSSLINKING IN TUMOR MAST CELLS

P.J. Millard, T.A. Ryan†, L.-M. Su, W.W. Webb§ and C. Fewtrell, *Departments of Pharmacology and Physics† and School of Applied and Engineering Physics§. Cornell University, Ithaca, NY.*

Digital video imaging microscopy of fura-2 fluorescence was used to monitor changes in intracellular free ionized calcium ($[Ca^{2+}]_i$) that occur upon crosslinking of IgE receptors on the surface of tumor mast cells. We have shown previously that the rapid increase in cytosolic calcium in stimulated rat basophilic leukemia (RBL) cells is preceded by lag times of varying duration (Millard et al. 1988. *PNAS.* 85:1854). When a field of cells is stimulated sequentially with the same or with different ligands both the latency and the fine structure of the calcium response are retained by each individual cell. In order to identify the source of the latency in the calcium response, RBL-2H3 cells were re-cloned by the limiting dilution method and the distribution of latencies of individual cells in the population were analyzed to determine whether genetic divergence could have given rise to the variation in latency. To see whether the typical distribution of cells in different stages of mitosis could affect the distribution of latencies, measurements of $[Ca^{2+}]_i$ were also performed using mitotically synchronized cells that had been selected by nocodozole pretreatment followed by a mitotic shake-off procedure. Neither recloning nor cell cycle synchronization affected the distribution of latencies of the calcium responses. Other potential reasons for the wide range of latencies and the unique nature of each single cell response are being studied currently.

Tu-Pos569

OPTIMIZED FLUORESCENCE DETECTION BY LASER SCANNING CONFOCAL MICROSCOPY (LSCM)

K.S. Wells, D.R. Sandison†, W.W. Webb, School of Applied and Engineering Physics, Department of Physics†, Cornell U., Ithaca, NY

In LSCM simultaneous focused illumination and confocal spatial filtering at the detector improve background rejection, signal-to-noise and axial resolution. Confocal spatial filtering exacerbates the limitations of optical information transfer due to fluorophore saturation, limited numerical aperture, imperfections in apochromatic optics and inefficiencies in the reflectance and transmittance along the optical train and in the detector. The conventional overall fluorescence photon detection efficiency of about 5% can be degraded to < 0.1% unless special care is taken in laser scanning confocal microscope design and operation. We find a natural optimum in confocal detector aperture size which maximizes the signal-to-noise ratio at a minimal cost in axial resolution, background rejection and signal levels.

Tu-Pos570

TWO-PHOTON EXCITATION IN LASER SCANNING MICROSCOPY

J. H. Strickler, W. Denk and W. W. Webb, Cornell U.

Simultaneous absorbtion of two red photons in a strongly focused stream of subpicosecond pulses from a colliding pulse mode-locked dye laser stimulates visible fluorescence from fluorophores having their normal absorption in the ultraviolet. The quadratic increase of the two-photon excitation rate with the excitation intensity restricts fluorescence emission to the focal volume. Intrinsic 3-d resolution in laser scanning microscopy is thus achieved. Photobleaching and most cellular photodamage are similarly confined to the focus, thereby minimizing sample degradation during 3-d image acquisition. Two-photon excited fluorescence images of living cells and other thick photolabile fluorescence labeled assemblies illustrate the depth discrimination of both two-photon fluorescence excitation and photobleaching. Even in these early experiments cellular photodamage was negligible.

The quadratic intensity dependence of two-photon excitation allows 3-d spatially resolved photochemistry, in particular, the photolytic release of caged compounds such as neurotransmitters, nucleotides and divalent cations. The two-photon release of caged ATP has been shown. Point photobleaching and a 3-d "write once read many" optical memory have also been demonstrated.

Tu-Pos571

FASTER IMAGING ACQUISITION IN SCANNING CONFOCAL MICROSCOPY VIA LINE ILLUMINATION

D.R. Sandison† and W.W. Webb, Department of Physics†, School of Applied and Engineering Physics, Cornell University, Ithaca, NY 14853

The rate of image acquisition in laser scanning confocal microscopes is limited by saturation of the excited state of fluorophore molecules in the focus of the scanning beam to one photon per fluorescence lifetime. Data collection rates may be increased by simultaneous illumination of many scanning confocal spots and parallel collection of the emission. To this end, we have proposed illumination by scanning with a focused line of light and detection by a linear diode array. The elements of the array collect signal from their conjugate object points simultaneously in this pseudo-confocal geometry, but the extended illumination does introduce excess background. The excitation intensity profile from a line of light is derived, and its effect on the x,y, and z resolution are presented. The results are compared to the case of point-illumination. The excess background due to non-conjugate illumination is calculated for line- and point-illumination.

Tu-Pos572

SIMULTANEOUS DIC AND FLUORESCENCE IN LASER SCANNING CONFOCAL MICROSCOPY

T. A. Ryan, D. R. Sandison, W. W. Webb, Cornell U.

Differential interference contrast (DIC) microscopy and laser scanning confocal fluorescence (LSCF) microscopy both provide very sensitive optical sectioning capabilities which allows one to probe the complex physico-chemical dynamics within individual living cells. In order to combine these two powerful techniques we have developed a method which allows for simultaneous acquisition of images using both methods. The intrinsic polarization of the laser excitation source, even after transmission through the scanning optics, is sufficient to obtain high resolution DIC images without introducing an additional polarizer in the epifluorescence pathway. The DIC image is collected in the transmitted light pathway equipped with appropriately oriented polarizer and recombining wollaston prism. We may thus achieve truly simultaneous imaging using both techniques with only negligible losses in the fluorescence pathway due to the introduction of the first wollaston prism. This method thus allows for efficient simultaneous acquisition of scanning DIC and confocal fluorescence images which should be useful in the study of the dynamics of biological processes within living cells.

Supported by the Developmental Resource for Biological Imaging and Opto-electronics funded by the NIH (RRO4224).

Tu-Pos573

Real-Time Detection of Electrical Activity in Cultured Neurons via Changes in their Intrinsic Optical Properties. R. A. Stepnoski*, G. E. Blonder*, F. Raccuia-Behling*, A. LaPorta*, R. E. Slusher*, and D. Kleinfeld. AT&T Bell Labs., Murray Hill, NJ 07974.

The scattering of light by neurons was used to detect individual action potentials in a single sweep. Cells with 10 - 15 μm diameter axonal segments were isolated from the abdominal ganglion of *Aplysia* and maintained in culture. They were illuminated with quasi-monochromatic light using darkfield optics. We detected light that was scattered by $> 4.5^{\circ}$ from a 200 μm diameter field that encompassed part of the axonal segment and many fine, regenerated processes. The normalized intensity of the scattered light was $I_{Scat}/I_{Incident} \sim 3{\cdot}10^{-3}$. A change in this intensity occurred during an action potential; $\Delta I_{Scat}/I_{Scat} \sim 3{\cdot}10^{-4}$. These changes were independent of the wavelength of the light (0.4 $\mu m \leq \lambda \leq$ 0.7 μm).

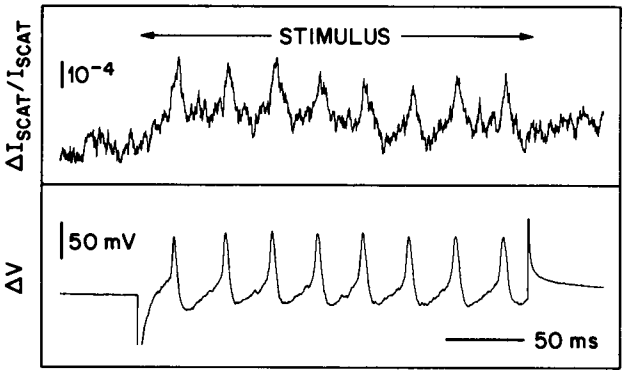

Tu-Pos574

SENSITIVE AND RAPID DETERMINATIONS OF FLUORESCENCE LIFETIMES IN THE FREQUENCY DOMAIN IN A LIGHT MICROSCOPE

R.M.Clegg, G.Marriott, B.A.Feddersen[1], E.Gratton[1], T.M.Jovin
Max Planck Institut f. biophys. Chemie, D-3400 Göttingen,FRG
[1]L.F.D., Dept. of Physics, Univ. of Illinois, Urbana, Il 61801, USA

An instrument to measure prompt fluorescence lifetimes in an image of a fluorescence microscope is described that employs a phase modulation method to determine the fluorescence decay parameters. The sample is excited by acousto-optically modulated laser light (UV and visible); the dispersion of the phase and modulation of the fluorescence signal extends over a frequency range of DC to 300 MHz. Any number of frequencies can be selected, depending upon the experimental objective. A usual experiment selects 20 frequencies over a 3 decade range centered about the expected lifetimes. The method is sensitive, the data can be rapidly and automatically acquired, and the performance characteristics are similar to the corresponding cuvette based fluorometer (only 10 minutes are required to measure 20 frequencies, and determine each phase to 0.1 degree, from a solution of 1 μM Rhodamine B).The technique can be used not only to measure the time decay of fluorescence from structures in biological and cellular samples, but also to measure the emission from microvolumes (submicroliter) of homogeneous solutions. Examples will demonstrate the versatility and the capabilities of the system.

Tu-Pos575

3-D RECONSTRUCTION OF SECRETORY GRANULES IN LIVING MAST CELLS BY FLUORESCENCE MICROSCOPY

T.J.Keating, R.A.Robb, and J.M.Fernandez, Dept. of Phys. and Biophys., Mayo Clinic, Rochester, MN 55905.

We aim to study the formation of intracellular organelles such as the secretory granules of mast cells. We have developed a personal computer-based workstation capable of reconstructing labeled organelles of living cells in 3-D. Giant secretory granules from beige mast cells (bg^J/bg^J) were fluorescently stained with 5-10 μM quinacrine and imaged using a Zeiss IM-35 inverted microscope and a Photometrics cooled CCD camera. Between 20 and 40 images were collected at 0.25 or 0.5 μm intervals from the bottom to the top of the cell. A micropositioning device (Heidenhain MT-25) which is sensitive to 0.5±0.1 μm displacements was used in conjunction with a microstepper motor (Daedal MC-2000) to move the objective lens (Zeiss Planapo 63x 1.4 NA) in controlled increments. The optical sections were deconvolved using the nearest-neighbors algorithm (Agard *et al.* (1988) Meth. Cell Biol. 30:353) to remove out of focus information. After deconvolution objects with an apparent size of ~0.25 μm were easily resolved. The filtering was done in the Fourier domain on a Mercury MC 3200 array processor operating in a Compaq Deskpro 386/25. The deconvolved optical sections of the cell were volume rendered using the software package Analyze® on a Silicon Graphics Personal Iris computer, connected via Ethernet to the acquisition/processing station. Several views of the cell were generated and, shown in succession, reveal the three-dimensional structure of the granules (a videotape will accompany our presentation). This technique will also be useful in immunofluorescence studies for the three-dimensional localization of specific structures.

Tu-Pos576

CONFOCAL AND DOPPLER MICROSCOPY OF CYTOPLASMIC STREAMING IN CHARA.

V CHEN, K.H.C.Associates,Amherst,NY

Major obstacles to the imaging and characterization of cytoplasmic streaming in Chara gobularis, a giant fresh water algae are 1)strong light scattering cell wall and chloroplast layers 2) intense auto-fluorescent chloroplast layer above the streaming tonoplast layer. We have been able to image clearly, through these layers, the streaming components with confocal light microscopy(4 frames/sec, single mirror scanning laser beam;30frames/sec.,scanning disk). We have been able to image through the calcium bands(in the case of banded cells) to show that chloroplasts under the band smaller and more intensely fluorescent than those in the inter-band region. Using laser Doppler microscopy we have followed changes in velocity distributions of the streaming components when the cell responds to stimulation. We have followed the velocity changes during NaCl induced oscillatory streaming.

Tu-Pos577

MANIPULATION OF SINGLE DNA MOLECULES IN A MICROSCOPE STAGE. M. F. Maestre, M. Miller, S. Goolsby, †W. Johnston, C. Bustamante*, Lawrence Berkeley Laboratory, Berkeley CA. and *Chemistry Dept. University of New Mexico. Supported by NIH Grants #AI08427 and GM #*GM32543, by the Director, Office of Energy Research, †Scientific Computing Staff, U.S. Dept. of Energy #DE-AC03-76SF00098 and by the LBL Human Genome Center.

A microelectrode chamber has been developed with a spatially distributed electrode network of microscopic dimensions. It was used in conjuction with a fluorescent imaging to permit the visualization and manipulation of a selected single DNA molecule, for the purposes of mechanical or chemical alteration of the molecule. The microelectrode net consists of 24 electrodes of dimensions of 10 microns in thickness with spacings between neighboring electrodes of 10 microns. The voltage of each electrode is controlled by a computer allowing the manipulation of the single DNA molecule on a microscopic scale. The images are continuously recorded for processing by image analysis programs. Single T4 bacteriophage DNA molecules have been manipulated and stretched to a full length of approximately 51 micrometers, very close to the reported length of 52 micrometers for the DNA of the related phage T2.

Tu-Pos578

Fourier Transform Image Processing to Extract Transport Coefficients from Video FRAP Measurements, Tsay, T-T., Inman, R.T., Jacobson, K.A., Dept. of Cell Biology and Anatomy, University of North Carolina at Chapel Hill, Chapel Hill, NC and Sun Microsystems, RTP, NC

One use of the fluorescence recovery after photobleaching (FRAP) technique is to measure the translational motion of membrane components. In a conventional FRAP experiment, a photomultiplier is used to measure the total brightness levels of the bleached region in the sample, so no spatial information can be obtained. In video-FRAP, a series of images is acquired of the spatial character of recovery using a video camera which allows direct detection of anisotropic diffusion and flow. To utilize all of the available data to determine the transport coefficients, the two-dimensional Fourier Transform is taken of the images after photobleaching. The change in the transform between two time points reflects the action of diffusion and/or flow during the interim; the diffusion equation predicts how each spatial frequency evolves in time. When the transforms at the two time points are divided, all information concerning the initial distribution of bleached fluorophores is removed, and the remaining information gives the diffusion coefficients directly. We discuss the systematic application this method to the diffusion of proteins as a function of image brightness (i.e. protein concentration). Preliminary work has shown that diffusion coefficients extracted from the Fourier analysis of video FRAP data agree with those obtained from conventional spot FRAP.

Supported by NIH GM 41402

Tu-Pos579

HIGH TIME RESOLUTION FLUORESCENCE IMAGING WITH A CCD CAMERA. N. Lasser-Ross, H. Miyakawa, V. Lev-Ram, S. Young, W.N. Ross Dept. of Physiology, N. Y. Medical Coll. Valhalla, NY 10595.

Scientific grade, cooled CCD cameras have many advantages for recording low-light level images. They have low noise, large dynamic range, no lag and high digital accuracy. However, a full picture usualy requires about 0.5 sec or more to be recorded. We have modified a standard Photometrics camera to record sequences of high speed images. These changes include using a frame transfer CCD chip, increasing the on-chip clock speed, and some software extensions to the commercially supplied instruction set. With these changes a 50X50 pixel image can be read every 25 msec; a 20x20 image can be read every 10 msec; pixels can be of variable size. We have used this system to make high speed fura images of calcium transients correlated with electrical activity in Purkinje cells in slices and leech neurons in culture. Calcium changes in individual dendritic twigs caused by single action potentials can be detected and separated from other events using an excitation intensity low enough so as not to cause significant bleaching or photodynamic damage.
Supported by the Whitaker Foundation, the NIH, and NSF.

Tu-Pos580

DETECTION AND CHARACTERIZATION OF MAGNETIC BACTERIA BY LIGHT SCATTERING IN A ROTATING MAGNETIC FIELD. Charles P. Bean and Augie Iadicicco, School of Science, Rensselaer Polytechnic Institute, Troy, NY 12180-3590.

Following Blakemore[1], we observe that magnetic bacteria in a rotating magnetic field will modulate scattered light. Earlier[2] we have given the rudiments of a theory of the rotation of bacteria. For quantitative measure we observe the scattering of laser (620nm) light by a bacterial suspension that is located in a region of uniform rotating magnetic field ($2 \leq \nu \leq 100$Hz, $B \leq 100$G). The characteristic frequency of the scattered light is twice that of the magnetic field. The output of a photodetector is measured by a lock-in detector at that double frequency. With this sensitivity we observe a magnetic signal in many natural surface waters. In contrast to Blakemore's original discovery, these objects are non-motile and exist in aerobic environments. In all cases, the bacterial specific enzyme lysozyme causes the signal to disappear. This is taken as evidence that they are magnetic bacteria-perhaps of a new class.

1. R.P. Blakemore et al, Geomicrobiol. J. 4, 53 (1984).
2. C.P. Bean, Biophys. J. 54, 258a (1989).

Tu-Pos581

ELECTROINJECTION IS AN EFFICIENT METHOD FOR INCORPORATING PROTEINS INTO LIVING CELLS. Allison K. Wilson and Primal de Lanerolle. Dept. of Physiology & Biophysics, Univ. of Illinois at Chicago, Chicago, IL 60612.

The introduction of nondiffusible probes such as antibodies and enzymes into living cells without compromising function is an important technique for studying cellular regulatory mechanisms. We have used a modification of the voltage discharge technique to introduce proteins into intact, viable cells (Biophysical J. 51: 214a, 1987). Electroinjection uses a relatively low field strength to transiently permeablize the plasma membranes of cells. We have further characterized this technique to demonstrate the cellular distribution of the incorporated protein and the effects of the protein concentration and molecular weight on incorporation. In addition, the uniformity of protein incorporation and the reproducibility of the technique was investigated. Our results demonstrate that electroinjection is simple, reproducible, and under carefully defined conditions, capable of introducing significant amounts of protein into large numbers of cells without decreasing cell viability or function.

Tu-Pos582

LASER DIODE LIGHT SOURCE FOR REAL-TIME INTERFEROMETRY IN THE ULTRACENTRIFUGE. Jeff Lary, Jia-Wen Wu and David Yphantis, Molecular and Cell Biology and Analytical Ultracentrifuge Facility, University of Connecticut, Storrs, CT 06269-3125.

Convenient real-time interferometry in the ultracentrifuge requires considerably higher light intensity than is available from the usual high pressure Hg arc lamps. Ideally the light source should exhibit moderate coherence and should be pulsed in synchrony with rotation of the ultracentrifuge rotor so as to provide "full contrast" interferometry and so as to make possible "multiplexing" of multiple cells. We have constructed a real-time interferometric system utilizing an inexpensive solid-state CCD camera as sensor and a laser diode emitting at 780 nm as light source. This diode is modulated to provide illumination only when the desired portion of the selected ultracentrifuge cell is properly positioned. Only several milliwatts (peak power) of illumination are adequate for good data acquisition. Supported by NSF grants DIR-8612159 and DIR-8717034.

Tu-Pos583

COPPER IODIDE STAINING AND DETERMINATION OF PROTEINS ADSORBED TO MICROTITER PLATES D. Root and E. Reisler, Mol. Biol. Inst.,Dept. of Chem. & Biochem., Univ. of Calif., Los Angeles, CA 90024

Copper iodide staining of proteins was first introduced as a highly sensitive, rapid, and inexpensive method for detecting proteins on nitrocellulose and nylon membranes (Anal. Biochem. 181, 250-253). This method is now extended to determinations of proteins adsorbed to polystyrene microtiter plates. The minimum amount of copper iodide stained protein detected in densitometric measurements is approximately 20 pg/mm^2. Enzyme immunoassay readers may also be used for these determinations albeit at lower sensitivity. The densitometric readings of copper iodide stained proteins vary linearly with the amount of protein present as verified by enzymatic and radioactive probes. Staining is complete in 2-3 min and may be removed by a 30 min treatment with EDTA without loss of adsorbed protein or immunoreactivity. The exact amount of protein adsorbed to microtiter plate wells can be measured by using protein bound and stained on nitrocellulose as a calibration curve.

Tu-Pos584

DETECTION OF CALCIUM-BINDING PROTEINS BY DIAGONAL ELECTROPHORESIS T. Otter and E. Hatch, Dept. of Zoology, Univ. of Vermont, Burlington, VT. (Intr. by P.A. Friedman)

To further our understanding of the role of Ca^{++} in controlling flagellar movement, we have developed a sensitive and reliable 2-dimensional electrophoresis method for detecting Ca^{++}-binding proteins (CaBPs) in flagella. After two successive orthogonal electrophoresis runs most polypeptides lie along a diagonal. However, when the second electrophoresis is run in the presence of Ca^{++} (50-200μM) the CaBPs lie off the diagonal in a region of low background staining. Their distance from the diagonal increases as $[Ca^{++}]$ is raised. Scallop sperm axonemes contain two CaBPs, one of which nearly comigrates with calmodulin (CaM). When Cd^{++} (similar ionic radius to Ca^{++}, ca. 1.0Å) is substituted for Ca^{++} in the second dimension, two distinct CdBPs are identified in addition to the CaM-like protein. Binding of Ca^{++} to CaM in this system is reversible. Diagonal electrophoresis offers several advantages over conventional gel methods for detecting CaBPs, e.g., better signal to noise ratio, larger mobility shift, semiquantitative measure of Ca^{++} affinity, and enhanced detection of minor bands.

Support: NSF DCB8812081 to T.O.

Tu-Pos585

PC-BASED DATA ACQUISITION FOR ANALYTICAL ULTRACENTRIFUGATATION. T.F. Holzman*, D. Egan, C. Chung, J. Rittenhouse, M. Turon.

A data acquisition/analysis system/software have been developed for analytical ultracentrifugation. The approach can be used with current (or future) analytical instruments. For the Model E, data acquisition and analysis is accomplished using the UV scanning system and PC-based A/D acquisition and analysis configured and programmed specifically for the task. The instrumentation can be used to acquire and analyze sedimentation equilibrium or sedimentation velocity data for as many as fifteen samples simultaneously. It is possible to perform direct modeling of protein-protein or protein-ligand association equilibria. The system is particularly useful for studying association behavior in systems exhibiting distributions of weight-average molecular weights. Constrained best-fit non-weighted sums of exponentials are calculated for observed distributions. The fitted exponential sums are used to analyze solution association behavior.

Tu-Pos586

ELECTRICAL SURVEILLANCE OF MAMMALIAN CELLS IN CULTURE. Charles R. Keese and Ivar Giaever, School of Science, Rensselaer Polytechnic Institute, Troy, NY 12180.

Mammalian fibroblasts are cultured on small gold electrodes carrying a weak AC current at 4000 Hz. When cells attach and spread on this surface, the impedance of the electrode increases by as much as a factor of 7 for a confluent layer depending on the cell line. The rate of this increase is strongly influenced by the type of protein adsorbed on the electrode. When the cells are in place, the impedance continues to fluctuate as a consequence of cell motion (1,2). Statistical analysis of the time course of these fluctuations shows they exhibit properties of a self-affine fractal. The data from both normal (WI-38) and transformed cells (WI-38/VA13) has been analyzed using Hurst's rescaled range analysis and is found to exhibit persistence, i.e. a "memory" of past fluctuations.

(These studies were conducted in part pursuant to a contract with the National Foundation for Cancer Research.)

1) Giaever, I. and C.R. Keese, PNAS, 81, 3761 (1984).

2) Giaever, I. and C.R. Keese, IEEE Trans. Biomed. Eng., 33, 242 (1986).

Tu-Pos587

A SUPERHETERODYNING MICROWAVE FREQUENCY-DOMAIN FLUOROMETER

E. Gratton & M. vandeVen. *UIUC, LFD, 1110 W. Green St., Urbana, IL 61801*

We have constructed a microwave frequency domain fluorometer with frequency range up to about 10 GHz. The detector is a 2 stage, 6 μm microchannel plate photomultiplier with a -3 dB bandwidth of 3 GHz and the light source is a picosecond cavity-dumped synchronously pumped dye laser. The signal at the detector consists of a series of harmonics spaced by 2 MHz extending up to several Gigahertz. Each individual harmonic is first converted to an intermediate frequency of 100 KHz. A second frequency conversion step reduces the frequency to 40 Hz where the phase and modulation of the harmonic frequencies is measured using digital techniques. This superheterodyning frequency translation greatly improves the sensitivity of the detector by decreasing the noise. Such a sensitivity increase extends the useful bandwidth of the detector to about 10 GHz. (Supported by PHS-P41-RR03155.)

Tu-Pos588

A NOVEL METHOD FOR THE DETERMINATION OF APPARENT DISSOCIATION CONSTANTS OF FLUORESCENT CALCIUM INDICATORS

Frank A. Lattanzio, Eastern Virginia Medical School, Norfolk, VA 23501

A ^{45}Ca-ion exchange resin system was used to overcome the limitations of calcium-EGTA buffers in measuring apparent dissociation constants (Kd) of fluorescent calcium indicators at acidic pH. 0.1M KCl buffered with 40 mM HEPES or MES was placed in stirred, thermostatted acrylic cuvettes. A ^{45}Ca/^{40}Ca admixture was then added, an aliquot removed for scintillation counting and then Chelex-100 was added. After 30 min, fluorescence was measured, fluo-3 added, fluorescence remeasured and a second aliquot removed for counting. From the corrected isotope measurements free calcium was determined, permitting calculation of the Kd and binding stoichiometry. The following Kds in nM were obtained at 37°C (n=6:mean±s.d.): pH 7.40=430±25; pH 7.00=552±23; pH 6.50=914±21; pH 6.00=1967±42; pH 5.50=6611±165. Similar trends were seen with indo-1 and fura-2 at 22° and 37°. Supported by an EVMS Institutional Grant.

Tu-Pos589

MECHANISMS AND KINETICS OF CRYSTALLIZATION OF HUMAN INSULIN.*

S. D. Durbin† and N. Rodriguez-Hornedo,††
†Physics Department, University of California, San Diego, La Jolla, CA and ††College of Pharmacy, University of Michigan, Ann Arbor, MI.

We have developed a procedure for the crystallization of recombinant human insulin in a system free of amorphous precipitate. By directly observing individual crystals, we have measured growth rates as a function of supersaturation. The rhombohedral four-zinc insulin crystals exhibited growth on all faces, although one set of symmetry-related faces grew faster than the opposing set. The dependence of growth rate on supersaturation followed the prediction for growth by a two-dimensional (2D) nucleation mechanism. However, electron microscopic studies of the surfaces of crystals showed features characteristic of both 2D nucleation and screw dislocation growth mechanisms at all supersaturations studied, with 2D nucleation becoming more important at higher supersaturation. These findings are similar to those for lysozyme.[1] In contrast, insulin crystals grown in the presence of precipitate grew predominantly by the dislocation mechanism, even at high supersaturation.

[1] S.D. Durbin and G. Feher, J. Mol. Biol., in press.

*Work supported by Eli Lilly and NIH.

Tu-Pos590

FREQUENCY- AND TIME-DOMAIN MEASUREMENTS OF PHOTON MIGRATION IN SCATTERING MEDIA AND TISSUE.

J.R. Lakowicz, K. Berndt, University of Maryland Medical School, Department of Biochemistry, Baltimore, MD, and M.L. Johnson, University of Virginia, Department of Pharmacology, Charlottesville, VA.

Recently, we reported on frequency- and time-domain measurements of photon migration in tissues [1]. These measurements indicated that the time-dependence of the reemerged light appears to be characterized by three parameters: 1) a delay time which depends on path length and detector geometry, 2) a sample transit-time spread which appears to depend on sample homo/heterogeneity, and 3) an exponential decay time which depends on sample absorbance and/or path length. In most practical measurements performed on living tissues, the sample is limited in space and/or contains heterogeneities like bones and blood vessels. In order to estimate the influence of these boundary conditions, we performed model experiments under well-defined conditions. A practically infinite sample was realized by increasing the sample volume up to 16 liter. These investigations have been made up by supplementary measurements on specially limited samples, and on samples containing defined heterogeneities. Finally, the results obtained by model experiments have been used to interpret measurements performed on human fingers, forearms, calfs and foreheads.

[1] J.R. Lakowicz, K. Berndt, and M.L. Johnson, Frequency- and time-domain measurements of photon migration in tissues, 1989 Annual Meeting American Society for Photobiology, Boston, MA, July 2-6, 1989. (From the Center for Fluorescence Spectroscopy, University of Maryland.)

Tu-Pos591

POSTSCRIPT AS A COMMAND LANGUAGE FOR LABORATORY INSTRUMENTS: APPLICATION TO A COMPUTER-CONTROLLED PATCH CLAMP.

H. Affolter[1] and F. J. Sigworth[2]
[1]Instrutech Corp, Elmont NY 11003 and [2]Dept. Cell. and Molec. Physiol., Yale School of Med., New Haven CT 06510.

Although Postscript is well known as a language for controlling laser printers, it is actually a general-purpose language that is optimized for controlling a computerized device from another computer. Following a suggestion by Dan Brown, we have implemented a Postscript interpreter (minus the graphics operators) for the EPC-9 patch clamp. Through the interpreter all functions can be controlled by simple statements; e.g.

```
1E9 SetCurrentGain
```

sets the current monitor gain to 10^9 volts/ampere, and

```
CSlow =
```

causes the present setting of CSlow to be returned as a string to the host computer. Thanks to standard features of Postscript, file operations, binary data transfers, macro-commands, loops and conditional statements can also be used. Entire programs can be down-loaded and executed in Postscript, freeing the host computer for other tasks.

Tu-Pos592

ASSESSMENT OF SKIN TEMPERATURE REGULATION BY DYNAMIC DIGITAL THERMAL IMAGING

J. Montoro, K. H. Lee, R. A. Spangler and M. Anbar

Sch. of Med. & Biol. Sci., SUNY, Buffalo

Skin temperature is regulated by several systemic and local mechanisms, the contribution of each varies in different areas of the skin and under different physiological and environmental conditions. Skin temperature changes with time by thermal oscillations superimposed on slow overall cooling or warming. This complex temporal behavior represents the summation of the different mechanisms involved. Using remote infrared sensing and digital image analysis we have repeatedly examined large areas of the skin at 8 sec intervals for 30 minutes. The temporal changes of different segments of the digitized thermal image were subject to Fast Fourier Transform analysis. Normal subjects and patients with known neurological disorders were studied under different physiological and environmental conditions. The findings will be presented and tentative mechanistic interpretations will be discussed.

Tu-Pos593

Gel-In-Matrix: A New Method for Immobilization and Extraction

R B Provonchee, T C Willis & F H Kirkpatrick, FMC BioProducts, 5 Maple St, Rockland, ME 04841

There is a large literature on methods for entrapment and manipulation of cells and other biological materials. Gelling polymers are widely used in these procedures. The resulting composites have found wide use in a few instances (top agarose; chromosomal DNA), but are limited in many uses by the diffusional barriers created by the gel coating or block. We have found a general method for retaining the advantages of entrapment while minimizing diffusional barriers.

In the simplest embodiment, cells or other biological materials are mixed with a suitable gelling agent (for example, low melting agarose or kappa carrageenan) and the liquid mixture is absorbed into polyurethane foam. After the mixture has gelled, the foam block is squeezed. Most of the water or buffer (80% or more) is expressed, and the gel is extensively fractured into small particles with dimensions similar to that of the cells in the foam. Other porous materials and fracturing techniques can be used.

Biological properties are unaffected, and the procedure is very gentle to cells. Red cells survive without significant hemolysis, yet can be rapidly hemolysed by passing distilled water through the fractured matrix. Entrapped yeast can be cultivated by flowing nutrient media through the block, with high ethanol production. Other examples will be given.

Tu-Pos594

FOURIER TRANSFORM METHOD FOR STATISTICAL EVALUATION OF CORNEAL ENDOTHELIAL MORPHOLOGY.

Barry R. Masters, Yim-Kul Lee and William T. Rhodes, School of Electrical Engineering, Georgia Institute of Technology Atlanta, GA 30332

The statistical evaluation of the shape, size, orientation, density and regularity of the corneal endothelial cells is an important diagnostic technique. The purpose of this research is to develop a novel hybrid optical/digital techniques to obtain the statistical measures in near real-time. Input test images were tracings of the cell boundaries from normal humans. The optical Fourier transform of each image was obtained and the radial projection and angular correlation function were plotted against angle and distance. The size of the cells could be obtained from the first peak of the radial projection versus radius. The width at half height divided by the peak radius was related to the coefficient of variation with respect to cell size. The separation between the peaks in the normalized angular correlation plot was related to cell shape. This method is suitable for the rapid evaluation of large numbers of endothelial images. **Support from NIH EY08402 (W. R.) and NIH EY-06958 (BRM).**

Tu-Pos595

POSITRON ANNIHILATION LIFETIME SPECTROSCOPY OF PROTEINS

Roger B. Gregory, Dept. of Chemistry, Kent State University, Kent, Ohio 44242.

When positrons enter condensed matter they rapidly lose their kinetic energy by collision until they reach thermal energies, at which point, some fraction form singlet or triplet e^+e^- bound states (positronium). The triplet state, or o-Ps, has a free-space lifetime of 140 ns, but this is reduced to 0.5 to 10 ns in condensed matter as a result of "pick-off" annihilation processes, in which an electron of appropriate spin from the medium is capture resulting in rapid subsequent annihilation. o-Ps lifetimes are therefore sensitive to electron density and polarizability and reflect the probability of Ps-electron encounters. o-Ps will be trapped in packing defects and regions of free volume. The fraction of o-Ps formed is a measure of the number of such sites, while o-Ps lifetimes measure the size of the free volume regions. Application of the technique to the study of proteins will be presented.

(Supported by NSF grant DMB 85-18941 and by Research Corporation).

Tu-Pos596

POLYMETHACRYLIC NANOPARTICULES USED AS BIOPHYSICAL VECTOR. **A. Allard and E. Rousseau* (Intro by J. Sygush). Dept. of Physiol./Biophys., Univ. of Sherbrooke, Sherbrooke, Que., Canada.**

The polymethacrylic nanoparticules (nP=0.3 μm ϕ) were developed as a new drug delivery system (Rolland et al. Int. J. Pharmac. 1989, 53). Doxorubicine (DXR) might interact with a 96% absorption yield on nP. DXR is also known to bind intracellular membrane proteins as previously reported (Zorzato et al., J. Biol. Chem. 1986, 261). Suspensions of nP-DXR complex were mixed with either i) SR membranes or ii) solubilized SR membrane proteins in 1.5% CHAPS + 0.5 M NaCl. Following incubation (1/2 h at 22°C), DXR was covalently bound to the proteins by UV-photolysis. SR membranes were solubilized as in ii. The nP-DXR-protein complex was sedimented. Non specific binding was assessed in presence of an excess of free DXR. Bound proteins were freed and revealed by SDS-PAGE. Both approaches yield similar results: a single high molecular weight protein band, ≈ 400 KDa, was consistently observed within the complex. Methodological improvements will be discussed and proposed for this promising system.

*A. A. was a fellow of ACIM; E. Rousseau is a Scholar of CHF.

Tu-Pos598

MICROSCOPIC MAPPING OF SUBNANOMETRIC MOTION. H. Lin and M. Sharnoff, Univ. of Delaware.

For several years we have had at our disposal a microscope-based holographic system capable, theoretically, of detecting motion of 10 Angstroms or less by objects well-resolved in the microscope. We have recently calibrated the system's sensitivity to motions of this size by observing the drifting of air bubbles introduced into a glycerine-filled glass capillary. The capillary was placed on the stage of our microscope with its axis nearly horizontal. A millimetric scale was set beside it, and observations made over several hours confirmed that the bubble trajectories were smooth and rectilinear. Drift velocities, ca 1 mm/hour, were different for bubbles of different diameter. The capillary and scale were illuminated by a laser beam at ca 30° to the horizontal, and the scattered light was collected through a 2.5X/0.08 objective and sent to a holographic plate. Difference holograms with interflash intervals as short as 2 msec were made. Images made from these holograms distinguish bubbles according to their velocities. A stationary bubble included in each scene gave a fixed reference point. Photos of the images, unenhanced by any electronic means, reveal absolute displacements as small as 11 Angstroms. Yet smaller relative displacements were also discernible.

Tu-Pos597

MEASUREMENT OF INTRACELLULAR FREE Ca^{2+} CONCENTRATION IN FRACTIONS OF ISOLATED GROWTH PLATE CHONDROCYTES USING FURA-2. M. Zuscik, R. Rosier, K. Gunter, E. Puzas and T. Gunter, Depts. of Biophysics & Orthopaedics, U. of Rochester, Roch., NY

Isolated avian growth plate chondrocytes convert the AM form of fura-2 quickly and completely to the FA form. This conversion is 65% complete in 40 min at 37°C. Control experiments showed that almost all of the converted indicator could be identified as intracellular fura-2FA and that the K_d of intracellular fura-2FA was very close to that at a similar ionic strength and pH outside the cell. A spectroscopic procedure was used to determine free cytosolic [Ca^{2+}] that corrects for errors which could be caused by Ca^{2+}-insensitive partial conversion products (found under some conditions of incubation) and fura-2 signals from the medium. Free cytosolic [Ca^{2+}] determined in freshly prepared chondrocyte suspensions containing all maturational stages varied over the range 75-95 nM. When cells from these various stages were separated by countercurrent centrifugal elutriation, the free cytosolic [Ca^{2+}] in the hypertrophic cells was four times higher than that in the resting cells.

Supported by GM35550, AR28420 & AR38945.

Tu-Pos599

MONTE-CARLO (MC) MODELING OF PHOTON TRANSPORT IN TISSUE (PTT) I. SIGNIFICANCE OF SOURCE-DETECTOR CONFIGURATION. Barbour, R.L., Graber, H., Lubowsky, J. (Intro. by Rushbrook, J.) Depts. of Path. and Biophysics, SUNY Health Sci. Center at Brooklyn, Brooklyn, NY, 11203.

Advances in the analysis of optical measurements of tissue will require the ability to infer the paths of scattered photons (SP) from directly measurable parameters. To examine these relationships we have modeled PTT by a MC simulation in a nonabsorbing, homogeneous, isotropic scattering medium. By examining the histories of SP we have determined the relationship between the intensity, I, of backscattered light (BL) and the average maximum penetration depth, <Z>, average number of collisions, <n>, and other non-observable parameters for photons emerging into selective detectors (D) for various source configurations. Results obtained showed that <Z> and <n> vary in a linear and quadratic manner, respectively, with distance, R, of D from a collimated point source (CPS). <Z> and <n> for SP emerging from media illuminated by a broad collimated or broad diffuse source had an angle dependence qualitatively similar to, but of much smaller magnitude than, that for a CPS. Unexpectedly, it was also determined that each D orientation has at least one "enantiomorph"; a second orientation at a different R with the same elevation angle but opposite azimuth, such that light received by both D has the same value of I, <Z> and <n>. These findings demonstrate that the subsurface properties of a random medium can be selectively interrogated by a position and angle scan of BL.

Tu-Pos600

MONTE-CARLO (MC) MODELING OF PHOTON TRANSPORT IN TISSUE (PTT) II. EFFECTS OF ABSORPTION ON 3-D DISTRIBUTION (3DD) OF PHOTON PATHS. Barbour, R.L., Graber, H., Lubowsky, J., and Aronson, R*. (Intro. by Brust, M.) SUNY at Brooklyn, and *Polytechnic Univ., Brooklyn, NY.

The attenuation of light by natural chromophores in tissue is one of the factors which determine the 3DD of the paths of emerging scattered photons (SP). In this study the effect of homogeneous absorption (HA) has on the intensity, I, avg. no. of collisions, <n>, avg. max. depth of penetration, <Z>, and on the 3DD of SP entering into selective detectors (D), was modeled by a MC method for photons experiencing isotropic scattering in a homogeneous medium. The efficiency of the MC simulation was maximized by considering the propagation of photon ensembles and employing techniques of correlated sampling, renormalization and Russian Roulette. Results obtained showed that an increase in HA produces an abrupt reduction in <Z> and <n> and a change in the functions relating them to distance, R, from linear and quadratic to square-root and linear, respectively. In addition, the dependence of <Z> and <n>, and hence 3DD, on the orientation of the D revealed that they vary markedly with elevation angle when the D are oriented towards, but not away from, the source. This dependence and the existence of enantiomorphic symmetry (see abst. #1 in this series) were present at all values of HA (0-10%). These results indicate that the ability to selectively probe the subsurface properties of a random medium are not diminished by the presence of HA but that the volume of medium contributing to the D response is reduced by an increase in HA.

Tu-Pos601

MONTE-CARLO (MC) MODELING OF PHOTON TRANSPORT IN TISSUE (PTT) III. CALCULATION OF FLUX THROUGH A COLLIMATED POINT DETECTOR (CPD) Barbour, R.L., Graber, H., Lubowsky, J., and Aronson, R*. (Intro. by Geetjens, E.) SUNY at Brooklyn, and Polytechnic Univ., Brooklyn, NY.

In this series (see abst. I and II) we have shown that the orientation and extent of detector (D) collimation are factors which influence the ability to selectively probe the subsurface properties of a turbid medium. Estimating the response of real D with narrow apertures, however, cannot be accomplished by conventional MC methods. Here we have applied the radiation transport equation (RTE) to the problem of determining angular flux (AF) through a CPD. Using an efficient MC method (see abst II), the detection of emerging flux through a CPD was determined by considering each collision site as the penultimate collision and randomly sampling a point along the acceptance axis for each CPD; thereby forcing the photons to contribute to the angular flux of all CPD. The scoring of AF, avg. max. depth of penetration, <Z>, and avg. no. of collisions, <n>, of the backscattered light entering through each CPD are derived from the RTE. Results showed that at a fixed distance from the source, <Z> and <n> are up to 4-fold less for a CPD oriented toward the source than for one with the opposite azimuth; the difference being greatest at surface-grazing elevation angles. This difference, and the presence of enantiomorphic symmetry (see abst. I) were found at all values of homogeneous absorption modeled. These results show that it is feasible to model responses of highly collimated D by a MC method.

Tu-Pos602

MONTE-CARLO (MC) MODELING OF PHOTON TRANSPORT IN TISSUE (PTT) IV. CALCULATION OF 3-D SPATIAL CONTRIBUTION TO DETECTOR RESPONSE (DR). Barbour, R.L., Graber, H., Lubowsky, J., and Aronson, R*. (Intro. by Lange, C.) SUNY at Brooklyn, and Polytechnic Univ., Brooklyn, NY.

Inferences about the subsurface properties of a random medium (e.g. tissue) will require an estimation of the 3-D distribution (3DD) of the paths of photons which contribute to the reponse of selective detectors (SD). For elastic scattering, a 3-D map of these contributing photons can be determined for any source-detector configuration as the product of collision density and the probability that a photon having a collision at this point will contribute to the DR. The former is directly calculated by a MC simulation. By employing a reciprocity theorem which considers the time reversal of photon paths entering a SD, the latter is determined through reinterpretation of a second 3-D collision density map as the 3-D map of expected contributions. In the limit of weak absorption, this product, called a "weight function" (WF), quantifies the absolute reduction in DR caused by absorption (A) at a given point in space. We have examined the dependence of WF upon the orientation of SD. Results obtained showed that while the volumes of medium having the greatest contribution to DR varied strongly with detector orientation, that lying beneath the receiver was most sensitive to these changes. Because the WF relates the DR to properties of specific volume elements, it can be used as the basis of methods for producing 3-D images of random media (e.g. tissue) from optical measurements.

Tu-Pos603

MONTE-CARLO (MC) MODELING OF PHOTON TRANSPORT IN TISSUE (PTT) V. MODEL FOR 3-D OPTICAL IMAGING OF TISSUE. Barbour, R.L., Graber, H., Lubowsky, J., and Aronson, R*. (Intro. by Ostashevsky, J.) SUNY at Brooklyn, and *Dept. of Physics, Polytechnic Univ., Brooklyn, NY.

The essence of any imaging technique requires that the detected signal be related to the properties of a particular volume in space. For multiple scattering media (MSM) a large number of, in principle infinitely many, voxels contribute to the detector (D) response in a nonlinear fashion which varies with the source-detector configuration (SDC); i.e. position and orientation of the D relative to the source. We have shown (see abst. IV in this series) that the 3-D distribution of these contributions can be calculated for any SDC. In this study we have developed a 3-D image reconstruction algorithm which employs weight functions (WF) in an unfiltered backprojection scheme. The attenuation (A) of backscattered light from a MSM, due to multiple (8) subsurface absorbers buried deep in the medium, corresponding to each SDC was calculated by a MC simulation for multiple source positions. Image reconstruction was accomplished by summing the products of the WF in each voxel and their corresponding A for all SDC and source locations. The resultant image, though convoluted, correctly resolved the 3-D horizontal and vertical boundaries and internal divisions of the absorber array. This study directly demonstrates that the reconstruction of 3-D images of subsurface structures buried at depths not visible from the surface in a random medium (e.g. tissue) is feasible.

Tu-Pos604

CONTRAST AND CHEMICAL SENSITIVITY IN SCANNING TUNNELING MICROSCOPE IMAGES OF DNA* S.M. Lindsay,[1] O.F. Sankey,[1] Y. Li,[1] C. Herbst,[2] and M. Philipp.[3] [1]Department of Physics and [2]Department of Chemistry, Arizona State University, Tempe, AZ 85287 and [3]Department of Chemistry, Lehman College, CUNY, Bronx NY 10468.

The scanning tunneling microscope (STM) can image large 'insulating' molecules. We present a tight-binding model of a molecule in a tunnel gap to show how tunnel conduction occurs when a vacant molecular orbital (MO) is brought into resonance with the metallic Fermi level. We present optical data to demonstrate how the tip-substrate-molecule interaction moves the energy of MO's in DNA by an amount which may permit resonant tunneling. The apparent 'height' of a feature in an STM image depends, among other things, upon the energy gap between the (unperturbed) MO and the metallic Fermi level. Thus the STM can distinguish molecules. Absolute identification is greatly simplified when target molecules are tagged in a manner which alters their electronic states substantially.

* Supported by the NSF (BBS8615653), ONR (N00014-87-0487), ASU and the PCS-CUNY Research Foundation.

Tu-Pos606

A SCANNING TUNNELING MICROSCOPE FOR BIOPHYSICAL RESEARCH L.D. McCormick,[1] D. McCormick,[2] U. Knipping,[3] and S.M. Lindsay.[3] [1]J&D Scientific and [2]Angstrom Technology, 1815 W. 1st Avenue, Mesa, AZ 85202 and [3]Department of Physics, Arizona State University, Tempe, AZ 85287.

The scanning tunneling microscope (STM) and atomic force microscope (AFM) can image biological molecules in water. Electrochemical techniques can be used to deposit molecules on a substrate uniformly. In addition, bioelectrochemical processes can be seen directly. Reaction products from the electrolyte may be studied at nanometer resolution. The STM has the advantage of chemical sensitivity because the tunnel current is sensitive to differences in electronic structure at the Å level. We are attempting to use this contrast to sequence DNA and RNA. We have developed an STM/AFM system for biological imaging (TAK 3.0) which incorporates an electrochemistry cell and potentiostat in the scanning head. Fast parallel processing with a transputer-based control system permits simultaneous acquisition, processing, display and storage of 16 bit data. We will illustrate the simplicity of operation with real-time demonstrations of molecular imaging under solution at the Angstrom Technology exhibit.

Tu-Pos605

ELECTROCHEMISTRY AS 'MOLECULAR TWEEZERS' FOR SCANNING PROBE MICROSCOPY* L.A. Nagahara, T. Thundat, P. Oden and S.M. Lindsay. Department of Physics, Arizona State University, Tempe, AZ 85287.

Scanning tunneling microscopy (STM) and atomic force microscopy (AFM) can be carried out in water. This means that it is now possible to use electrochemical methods to bind molecules to a substrate. In the right conditions, it is possible to cover a surface with an adsorbate layer that is uniform (on a nm^2 scale) over mm^2 areas, eliminating the need to hunt for suitable images. Three electrode control of the surface charge on a substrate permits investigation of molecular binding mechanisms and allows various substrates to be used to bind a particular molecule.

We will present images of a variety of nucleic acids which illustrate bioelectrochemical processes directly, and reveal nanometer scale structure in the hydrated material for the first time.

* Supported by the NSF (BBS8615653), ONR (N00014-87-0487) and ASU.

W-AM-Sym I-1

STRUCTURAL DATABASES IN PROTEIN MODELLING AND DESIGN

T. Alwyn Jones, Department of Molecular Biology, BMC, Box 590, S-751 24 Uppsala, SWEDEN

Protein molecules adopt limited energetically preferred conformations. One approach to modelling is therefore to restrict, force, or persuade users to work with these preferred conformations. This can be implemented with databases for side chains and main chains and can help identify sequence dependent conformations. Cluster analysis of protein structures allow the use of a limited subset of fragments for most modelling purposes. These fragments contain little single residue sequence dependence on structure.

W-AM-Sym I-2

ZINC FINGERS

Jeremy M. Berg, Department of Chemistry, The Johns Hopkins University, Baltimore, MD 21218

In recent years a large family of gene regulatory proteins has been discovered that is characterized by the presence of one or more sequences of the form (Tyr,Phe)-X-Cys-$X_{2,4}$-Cys-X_3-Phe-X_5-Leu-X_2-His-$X_{3,4}$-His. Each of these sequences appears to bind a zinc ion via the invariant cysteine and histidine residues to form a small structural domain that has been termed a "zinc finger". A prediction for the three-dimensional structure of these domains was developed based on the discovery of recurring substructures in crystallographically characterized metalloproteins. The structure consists of a two stranded antiparallel beta sheet followed by an alpha helix. The three highly conserved hydrophobic residue pack together to form a hydrophobic core adjacent to the metal coordination unit. Recent experimental results have revealed that this prediction is essentially correct. The knowledge of the structure of single domains has allowed development of models for the structures for arrays of tandemly repeated domains which is the form active in site-specific DNA binding. These models make strong predictions about the mode of interaction between the zinc finger proteins and nucleic acids.

W-AM-Sym I-3

STRUCTURE OF ALPHA1-12, A DESIGNED SYNTHETIC PROTEIN MODEL.

David Eisenberg, Christopher P. Hill, Daniel H. Anderson & Morgan Wesson, Molecular Biology Institute, UCLA, Los Angeles, CA 90024 & William F. De Grado, Central Research & Development, E.I. du Pont de Nemours & Co., Wilmington, DE 19898. **X-ray diffraction reveals that the structure of a designed protein model is more complex than the design. The structure is formed from non-covalent self-association of a 12 residue fragment of a longer peptide designed to form an amphiphilic α-helix with a ridge of Leu residues along one helical face; by interdigitation of the leucines of four such helices, the design called for self-association of four helices into a structure of the four α-helical bundle class. In the actual structure, α-helical tetramers are present, but there are also hexamers with a hydrophobic core of 12 leucine residues. These results indicate that it may be easier to design an amino acid sequence that folds into a compact protein-like packing than to design a specific folding pattern.**

W-AM-Sym I-4

Abstract : Antibody combining sites : prediction and design

Dr. Anthony R. Rees*, Andrew C.R. Martin, David Webster, Janet C. Cheetham and Sally Roberts

* on leave at IGEN, Inc. Rockville, MD USA from Laboratory of Molecular Biophysics, University of Oxford, England)

Algorithms for predicting the three-dimensional structure of CDRs from sequence data alone are being developed by several laboratories. Some procedures are based on the so-called maximum overlap method (MOP) and have been used independently by a number of groups whose approaches differ in the way in which CDR loops are selected as starting points. In general, modeling by homology alone is not reliable enough to generate the correct conformation of all CDRs even when the procedures incorporate the "key residue" modifications of Chothia and Leak. We have developed a general solution to the prediction problem which combines the resource of the complete protein structure database (the knowledge based component) with conformational search algorithms (the ab initio component) and which requires no arbitrary decisions to be made by the operator. Details of the methodology and of recent developments will be presented.

In addition, progress in the development of algorithms that enable the user to dock the epitope on the surface of an antigen to its antibody combining site by a computational procedure will be discusssed. This requires some knowledge of those antibody residues involved in antigen contact. The manner in which protein engineering can be used to supply this information will be described.

W-Am-Sym II-1

ADRENERGIC RECEPTORS: ASSOCIATION OF SPECIFIC FUNCTIONS WITH DEFINED STRUCTURAL MOTIFS. M. G. Caron and R. J. Lefkowitz, Dept. of Cell Biol., Med., and Biochem., HHMI, Duke Univ. Med. Ctr., Durham, NC

The primary structure of all major types of adrenergic receptors (AR) (β_1, β_2, α_{1B} and α_{2A}) as well as several newly characterized subtypes (α_{2B}, α_{1A} and α_{1C}) has been elucidated by the cloning of their genes and/or cDNAs. These receptors all possess the now familiar seven hydrophobic transmembrane domains characteristic of G-protein coupled receptors. The ligand binding site of these receptors appears to reside within the hydrophobic pocket created by the transmembrane helices, but disulfide bounded cysteines in hydrophilic extracellular domains may participate or stabilize the ligand binding site. By mutagenesis we have identified both ends of the third cytoplasmic loop proximal to the membrane and the amino terminal region of the carboxy tail as being involved in the G-protein activating function. Phosphorylation of βAR by PKA and the βAR kinase on cytoplasmic sites appear to be important to regulate the function of βAR. Elucidation of the structural determinants of receptor function should help in understanding the mechanisms of signal transduction and regulation.

W-Am-Sym II-2

SELECTIVITY OF RECEPTOR-G PROTEIN COUPLING. E. M. Ross, S. K-F. Wong, E. M. Parker and T. Higashijima. Dept. of Pharmacology, Univ. of Texas Southwestern Medical Center, Dallas, TX 75235-9041.

Chimeric receptors and receptor-mimetic peptides have been used to define domains on the cytoplasmic surface of G protein-coupled receptors that determine regulatory activity and selectivity among G proteins. Replacement of the third cytoplasmic loop of the M1-muscarinic receptor with homologous sequence from β-adrenergic receptors confers regulation of G_s, but without abolishing regulation of G_p. The relevant region consists of six amino acids near the N-terminal end of the loop. Replacement of sequence in the second loop had little effect by itself but, when coupled with replacement of the third loop, markedly decreased coupling to G_p and maintained coupling to G_s. Replacements in the C terminal domain can enhance stimulation of G_p but have not caused obvious changes in selectivity. Regions important for selectivity are cationic and are amphiphilic when modeled as α helices. Peptides with similar charge distributions also regulate G proteins with characteristic selectivities or inhibit regulation, providing low molecular weight models for regulatory structures.

W-Am-Sym II-3

CALMODULIN DEPENDENT PROTEIN KINASES IN SMOOTH MUSCLE AND ITS ROLE OF THE REGULATION ON CONTRACTION. M. Ikebe, Dept. of Physiol. and Biophys., Case Western Reserve Univ.

The role of Ca^{2+} in regulating smooth muscle contraction involves the activation of Ca^{2+}/calmodulin dependent protein kinases. Myosin light chain kinase (MLCK) phosphorylates 20 kDa light chain of smooth muscle myosin and this triggers the activation of the contractile apparatus. The regulatory mechanism of smooth muscle MLCK has been investigated and it is proposed that the inhibitory region and calmodulin binding region lie next to each other. The possible interaction of the regulatory site and the catalytic site of MLCK will be discussed. Although it is known that the phosphorylation of myosin by MLCK activates actomyosin, the molecular mechanism of the activation is still obscure. The possible mechanism will be discussed. Our recent study using isolated single smooth muscle cells suggested that Ca^{2+}/calmodulin dependent protein kinases may be involved in the Ca^{2+} homeostasis of the smooth muscle cell. We purified Ca^{2+}/calmodulin dependent multifunctional protein kinase from smooth muscle, and the possible role of this kinase in Ca^{2+} homeostasis was examined. Furthermore, the role of this kinase on caldesmon function was studied. (Supported by NIH, AHA, and Syntex).

W-AM-Sym II-4

cAMP-DEPENDENT PROTEIN KINASE: STRUCTURAL FEATURES OF AN ENZYME FAMILY. **S. S. Taylor J. Buechler, W. Dostmann, W. Yonemoto, Chemistry Dept., University of California, San Diego, La Jolla, CA 92093, U.S.A.**

Although the eukaryotic protein kinases represent a large family of diverse enzymes, each retains a highly conserved catalytic core. A combination of chemical, recombinant, and crystallographic approaches were used to probe the active site regions and overall structure of cAMP-dependent protein kinase (cAPK), one of the simplest of the protein kinases. cAPK serves as a framework for establishing many of the features that will ultimately be important for all protein kinases. The roles of Lys 72, a glycine-rich loop, and Asp 184 in ATP binding and catalysis in the catalytic subunit (C) are invariant features of every kinase. In contrast, many features of the peptide recognition site vary for each kinase. In the absence of cAMP, C is maintained in an inactive state by aggregation with the regulatory (R) subunit. The inhibitory properties of R are localized at a proteolytically sensitive hinge region that resembles a substrate peptide. The R-subunit has a well-defined domain structure and mutant proteins lacking the N-terminus as well as both cAMP binding domains have been constructed. Using these deletion mutant proteins plus single amino acid substitutions, a model for the cooperative activation and reassociation of the holoenzyme is proposed.

W-AM-Sym II-5

IONIC CHANNEL NETWORKS FORMED BY G PROTEINS.

A.M. Brown†, A. Yatani†, J. Codina‡ and L. Birnbaumer‡, Departments of Molecular Physiology and Biophysics†‡ and Cell Biology‡, Baylor College of Medicine, One Baylor Plaza, Houston, TX 77030.

Ionic channels comprise the largest class of membrane effectors for G proteins presently known. G proteins act on ionic channels via cytoplasmic second messenger (indirect) or membrane-delimited (direct) pathways. Although specific intermediaries have not been excluded from the direct pathway, membrane enzymes that are known G protein effectors such as adenylyl cyclase, can be excluded. Direct G protein effects are either essential to channel opening (obligatory) e.g., atrial muscarinic K^+ channels, or secondary to changes in membrane potential (modulatory) e.g., dihydropyridine-sensitive Ca^{2+} channels, and Gα subunits mediate these direct effects. The idea that one type of G protein couples to only one type of effector is not supported. Preactivated α_s may have Ca^{2+} and Na^+ channels and adenylyl cyclase as effectors and preactivated α_i may have more than one effector including an ionic channel. Thus, G proteins spatially organize membrane effectors into networks. The networks are flexible because more than one activated Gα molecule can cycle through one receptor or one effector. The networks are also organized temporally by direct and indirect G protein pathways to produce fast and slow responses.

W-AM-Sym II-6

SITE-DIRECTED MUTAGENESIS ON VOLTAGE-GATED CHANNELS

Walter Stühmer, Max-Planck-Institut für biophysikalische Chemie, 3400 Göttingen, FRG.

After deducing the complete amino-acid sequence of the voltage-gated sodium and potassium channels by cloning and sequencing the complementary DNA, primordial interest rests on identifying the main functional regions such as the voltage sensors, regions involved in the inactivation, the pore-forming segments and the binding sites for toxins such as TTX and STX. Site-directed mutagenesis on the sodium channel has shown that charged residues in the S4 segment are involved in the potential-dependent activation process. Also, an intracellularly located region between repeats III and IV is crucial for inactivation, since modifications in this region affect inactivation. A single point mutation in a region thought to be extracellular according to current topological models is able to reduce the affinity for TTX and STX by more than three orders of magnitude. There are several lines of evidence indicating that this location is situated in close proximity to the channel pore. Due to the high homology between all potential dependent channels, these findings might apply to all of them.

W-PM-Sym 1

THE EFFECTS OF SEQUENCE, CHEMICAL MODIFICATIONS, AND SOLVENT ON THE STRUCTURES OF NUCLEIC ACIDS

Helen M. Berman, Department of Chemistry
Rutgers University, New Brunswick, NJ

The structures of nucleic acids are affected by sequence, solvent and chemical modifications. Our analyses of nucleic acid structures have begun to reveal the nature of sequence dependency of the solvent networks. Similar analyses of the effects of chemical modifications of the bases show, that of the structures thus far determined by crystallographic methods, none show changes in the global structure although there are subtle but definite effects on the local conformations. On the other hand, the properties in solution are greatly affected by these changes. These properties may be related, in part, to changes in the hydration structure. The implications of these changes and the relationships between solution and crystal properties will be discussed.

This work has been supported by grants from the NIH: GM 21589, CA 06927, RR 05539.

W-PM-Sym 2

STRUCTURE AND ENERGETICS OF OLIGONUCLEOTIDES CONTAINING UNPAIRED BASES IN AN OLIGO(dA)•OLIGO(dT) TRACT.

Kathleen M. Morden, Dept. of Biochemistry, Louisiana State University, Baton Rouge, LA 70803

A series of oligonucleotide duplexes which contain an unpaired base in the center of an $A_4 \cdot T_4$ tract have been investigated as a model for a frameshift mutation. The global structures of these duplexes have been determined using one-dimensional and two-dimensional NMR. Evidence for both the intrahelical and extrahelical conformations will be presented. The structure of the central A•T region is itself unusual and the effect of the unpaired base on this structure has been probed using primarily NOE interactions. The temperature dependence of these structures has also been investigated.

Thermodynamic parameters for these perturbed duplexes have also been determined. The enthalpy, entropy and free energy for duplex formation in the presence of an intrahelical or extrahelical base will be compared with results obtained for the unperturbed duplex. These thermodynamic results will be correlated with the structural information obtained from the NMR studies.

Supported by N.I.H. Grant GM38137 and Louisiana Education Quality Support Fund LEQSF(86-89)-RD-A-12.

W-PM-Sym 3

CONFORMATION OF VIRAL DNA STUDIED BY RAMAN SPECTROSCOPY.

R. Becka, S. Towse and G. J. Thomas, Jr., Div. Cell Biol. & Biophys., School of Basic Life Sciences, University of Missouri - Kansas City, Kansas City, MO 64110.

The Raman spectrum of DNA exhibits bands which are diagnostic of backbone phosphodiester geometry and nucleoside furanose pucker. The spectrum also contains information related to base stacking geometry, helix groove dimensions and higher order DNA configurations. We have studied DNA and RNA crystals of known three-dimensional structures to establish quantitative and detailed correlations between the Raman spectrum and nucleic acid conformational parameters. Using these correlations, the structure of DNA in aqueous solution, in complexes with regulatory proteins, and in packaged viral chromosomes may be probed effectively by static Raman methods. The DNA structure information can be significantly enhanced when these static methods are augmented by a Raman dynamic probe of solvent access to the exchangeable groups lining the major groove of double helical DNA. Results obtained from viruses which package dsDNA will be discussed. [AI 18758]

W-PM-Sym 4

METASTABLE STATES OF RELAXED SUPERCOILED DNAS.

J. M. Schurr, P.-G. Wu, L. Song, and B. S. Fujimoto, Department of Chemistry, University of Washington, Seattle, WA 98195.

It is widely supposed that the global secondary structure of native supercoiled DNA is derived from that of its equilibrium linear DNA (generic B-helix) by simple strains and that, upon release of the superhelical stress, it coasts rapidly down the strain potential surface to reach that equilibrium state. However, some evidence suggests that non-simply strained (i.e. alternate) global secondary structures may prevail in supercoiled DNAs, and a variety of observations indicate that some fraction of the sequence remains trapped in a metastable state after the superhelix density is completely relaxed by linearization, by intercalated dyes, or by the action of Topoisomerase I. The metastable state exhibits a lower torsion constant than either the native supercoiled or equilibrium linear DNA, and may take two months or more to equilibrate. Partial relaxation of the superhelix density by E. coli single strand binding protein also yields a state with low torsion constant that may be stable. Studies as a function of superhelix density provide some evidence for the implied transitions in equilibrium secondary structure as the superhelix density is varied from native to zero. The range of these transitions appears to be extensive, if not global.

W-PM-Sym 5

PROGRESS IN PREDICTING RNA STRUCTURE

Douglas H. Turner (Intro. by Victor Bloomfield), Department of Chemistry, University of Rochester, Rochester, NY 14627

Thermodynamic studies on oligoribonucleotides provide parameters that can be used to predict RNA secondary structure with free energy minimization algorithms. Parameters for interactions determining three dimensional folding can also be derived. Recent results for oligoribonucleotides and for a self-splicing RNA will be presented. Comparisons of structures derived from free energy minimization and from phylogeny will also be discussed. With the current data base, it appears that on average roughly 70% of the secondary structure of an RNA can be predicted from sequence.

W-PM-A1

POLYMORPHISM OF 2D CRYSTALS OF THE MITOCHONDRIAL CHANNEL, VDAC: IMPLICATIONS FOR CONFORMATIONAL CHANGES IN THE CHANNEL PROTEIN. C.A. Mannella, X.W. Guo, H. Chen, Wadsworth Center, NYS Dept. of Health, and Depts. of Biomedical Sciences and Physics, State Univ. of NY, Albany, NY.

Crystalline arrays of the VDAC channel induced by phospholipase A_2 in Neurospora mitochondrial outer membranes are polymorphic. In the more oblique parallelogram array, there are large, channel-free areas occupied by protein "arms" that extend between the channels (seen by cryo-electron microscopy of unstained, frozen-hydrated membranes). These arm-containing regions are absent in contracted forms of the VDAC crystal, indicating an altered conformation of the arms. We have found that effectors of the voltage dependence of the VDAC channel, an amphipathic polyanion and aluminum, induce changes in the crystal form and lattice order of the VDAC arrays. This suggests that the gating process may involve (or be strongly effected by) the interactions of the protein arms with the membrane bilayer and with other parts of the channel protein. (Supported by NSF grant DMB-8613702.)

W-PM-A2

PROBING THE STRUCTURE OF THE VDAC ION CHANNEL BY SITE-DIRECTED MUTAGENESIS. M. Forte*, E. Blachly-Dyson*, S. Peng# and M. Colombini# *VIABR, Oregon Health Sciences University, Portland, OR 97201; #Department of Zoology, University of Maryland, College Park, MD 20742.

VDAC is a small protein of the outer mitochondrial membrane that forms large, weakly anion selective, voltage-gated pores on incorporation into planar lipid bilayers. Using site-directed mutagenesis, over 40 single and multiple mutations were introduced into the yeast VDAC gene to change the charges of amino acids at specific positions. The mutant genes were expressed in yeast cells lacking the VDAC gene, mutant proteins purified and introduced into bilayers for biophysical study. All of the mutations produced channels with single channel conductances similar to the wild-type protein indicating that the channels were essentially normal. Many of the mutations altered the channel's open state ionic selectivity. These residues are likely to line the walls of the channel in the open state. Initial studies indicate that a subset of the residues that affect open state selectivity do not affect closed state selectivity. Study of these mutant channels will help us elucidate the conformational changes required for channel opening and closing (supported by NIH grant #GM35759 and ONR grant #N00014-85-K-0651).

W-PM-A3

PROBING FOR THE VOLTAGE SENSOR IN THE MITOCHONDRIAL CHANNEL, VDAC, USING SITE-SPECIFIC MUTAGENESIS

*Lorie Thomas, +Elizabeth Blachly-Dyson, *Marco Colombini and +Mike Forte
*University of Maryland, College Park, Maryland 20742
+Oregon Health Sciences University, Portland, Oregon 97201

VDAC is a voltage-dependent channel found in the mitochondrial outer membrane of all eukaryotic kingdoms. The channel is in a high conductance state (open) with no or low membrane potentials and adopts low conductance states (closed) in the presence of small (>20 mV) transmembrane potentials. Analyses of the voltage dependence and conformational energy of the channel for single amino acid substitutions in the protein were performed by fitting the conductance-voltage curves to the Boltzmann distribution. The data for the transition from the open to closed state can be fit quite well to a two state approximation. For mutants which displayed decreased voltage dependence, dextran sulfate (Mangan and Colombini, PNAS 1987), which increases the voltage dependence of the channel with little change in the energy difference between the states, was added so that channel closure might occur within the voltage range that could be examined. A glutamic acid substituted for a lysine in position 19 from the N-terminus resulted in 2.5 fold reduction in the steepness of voltage dependence when compared to wild type VDAC under the same conditions. By contrast, the same substitution at positions 132, 205, 211, and 248 did not alter the steepness of the voltage dependence. (Supported by ONR grant #N00014-85-K-0651 and NIH grant #GM35759)

W-PM-A4

LOWERING THE pH GREATLY ENHANCES VOLTAGE-DEPENDENCE OF MITOCHONDRIAL PORIN CHANNEL. L.Ermishkin and T. Mirzabekov (Intro.by C.A.Mannella) Institute Biological Physics of Acad. Sci. Pushchino, USSR, 142292

The effect of pH on properties of mitochondrial porin channels in a lipid bilayer has been studied. The channel is shown to have several states of different conductance and selectivity. Steepness of the voltage-dependence of the probabilities of different states sharply increases at pH 3 where negative charges of Asp and Glu are neutralized. It is concluded that the channel gate is controlled by a great number of negative and positive charges. High steepness observed at low pH suggests at least 60 positive charges to participate in controlling the channel gate. In other words almost all amino groups of channel-former must pass through the entire membrane voltage upon random motion of the channel among the states. These results support the conclusion that channel closing leads to redistribution of the electric field within the pore (Colombini, J Theor Biol.110:559; 1984)

W-PM-A5

PARAMECIUM MITOCHONDRIA CONTAIN THREE DIFFERENT OUTER MEMBRANE CHANNELS. R. Benz[a], A. Schmid[a], and J.E. Schultz[b], [a]Lehrstuhl fur Biotechnologie, Univ. Wurzburg; bPharmazeutisches Inst., Univ. Tubingen, (F.R.G.)

Isolated Paramecium mitochondria were treated with a Genapol containing buffer. Most of the outer membrane was dissolved by this treatment and the dissolved material was applied to a hydroxyapatite column. Two pore-forming proteins were found in the eluate of the column. The normal mitochondrial porin with a mol. wt. of about 35 kD eluted shortly after the void volume. It formed in the "open" state a slightly anion-selective channel with a single-channel conductance of about 2.4 nS in 1 M KCl. Further elution of the column with a buffer containing 0.1 M KCl resulted in the appearance of a low mol. wt. protein which formed a highly anion-selective channel in lipid bilayer membranes with a conductance of 0.8 nS in 1 M KCl. The supernatant of osmotic shock-treated mitochondria contained the third pore with properties which were very similar to those observed recently in porin-free yeast mutants. This pore had a short lifetime and a single-channel conductance of 2 nS in 1 M KCl.

W-PM-A6

CHARACTERIZATION OF MAMMALIAN AND YEAST MITOCHONDRIAL CATIONIC CHANNELS.

J.P. HENRY, J.F. CHICH, F. FEVRE[1], D. GOLDSCHMIDT[2] & M. THIEFFRY[1]. (Intro. by R.T. KADO). I.B.P.C., 13 rue P. et M. Curie, 75005 Paris, [1]C.N.R.S. Gif sur Yvette and [2]C.N.R.S. Villeurbanne, France.

A cationic channel of large conductance is observed in tip-dip bilayers enriched in bovine or rat mitochondrial membranes. The channel is sensitive to trypsin externally applied to intact mitochondria and is more abundant in fractions enriched in outer membrane. It is partially solubilized by digitonin, suggesting a possible localization on contact sites.

A voltage-dependent channel of large conductance was also observed in yeast mitochondria. It differs from VDAC since the same channel was found in porin-deficient mutants. It has the same cationic selectivity as the mammalian channel. Both mammalian and yeast channels are blocked in the same way by an addressing peptide with the sequence of pCOXIV(1-12). These data suggest that the cationic channels from mammalian and yeast mitochondria are related forms of the same channel. The blockade properties are consistent with a translocation of the peptide through the channel.

W-PM-A7

CHANNELS IN MITOCHONDRIAL CONTACT SITES. °O.Moran, +G.Sandri, +E.Panfili, xW.Stühmer, and M.C.Sorgato. °ISAS,Trieste-Italy; +Dept. of Biochemistry, Trieste-Italy; xMPI für biophysikalische Chemie, Goettingen-FRG; *Dept. of Biochemistry, Padova-Italy.

The patch clamping of liposomes containing a fraction enriched in contact sites between the two membranes of brain mitochondria reveals the presence of 3 levels of conductance. The lower comprises groups of channels of approx. 10 and 30 pS conductance. The second a channel of 475 pS with 2 distinct subconductance states (245 and 373 pS). The third, conductances ranging from 550 pS to approx. 1 nS. Apart from the first group, found also in the isolated mitochondrial membranes, the other channels seem to reside preferentially in the contact sites fraction. Contrary to the 107 pS channel, originally found in mitoplasts, and to the outer membrane anion channel, contact sites channels are voltage independent, and thus can be open at physiological ψ sustained by mitochondria. The methods used for their isolation and reconstitution into liposomes seem not to be the cause for loss of voltage sensitivity. In fact voltage gated channels are found in proteoliposomes containing either the isolated outer membrane or a partially purified fraction of the inner mitochondrial membrane.

W-PM-A8

AN EFFECT OF Ca^{2+} ON THE CHANNEL ACTIVITY OF THE MITOCHONDRIAL INNER MEMBRANE. K.W. Kinnally*#, S. Perini* and H. Tedeschi*, *Dept. Biological Sciences, SUNYA and #Dept. Biology, Siena College, Loudonville, N.Y.

Sorgato et al. (1987, Nature 330:498-500) observed in mitoplasts in 150 mM KCl a slightly anion selective channel of 107 pS which closes at negative potentials. An additional 350 pS channel was attributed to the outer mitochondrial membrane. We have reported multiple conductance levels and the ion selectivity of three of these (Kinnally et al., 1989, J. Bioenerg. Biomembr. 21:497-505). In the present study, when the mitochondria were isolated in sucrose media, we usually detected channel activity as we previously reported and without the presence of the channel of Sorgato et al. (1987). However, after treatment with EGTA we have observed this channel (~ 110 pS, closing at negative potentials) regardless of Ca^{2+} concentration. The other conductance levels were observed less frequently after EGTA treatment. Frequently, the patch resistance increased with Ca^{2+}, particularly in the negative range of potentials.

Supported in part by NSF grant DCB 8818432.

W-PM-A9

THE GIANT CHANNEL OF THE MITOCHONDRIAL INNER MEMBRANE. M. Zoratti, V. Petronilli and I. Szabo', CNR C.S. Fisiologia Mitochondri, Dept. Biology, University of Padova, Italy (Introduced by K.W. Kinnally).

Patch-clamp experiments on rat liver mitoplast membranes revealed the presence of a giant channel with a maximal conductance of about 1.3 nS in 150 mM KCl. It possesses a variety of substates, ranging upward from values of 0.3 nS (or possibly lower). Operation of the channel in one of these substates, rather than in its maximal conductance state, is favored by higher positive (on the matrix side) applied transmembrane voltages. Some characteristics of the channel suggest that it is not the outer membrane porin (VDAC). It resembles instead the mechanosensitive channels reported to exist in the cytoplasmic membrane of both gram-negative and gram-positive bacteria[1-3], and the channel recently found in the rough endoplasmic reticulum[4]. While its function remains unknown, an involvement in transmembrane protein transport appears likely.

[1]Martinac, B. et al. (1987) PNAS USA 84:2297-2301; [2]Zoratti, M. & Petronilli, V. (1988) FEBS Lett. 240:105-10; [3]Zoratti, M. et al. & Berrier, C. et al., in press; [4]Simon, S.M. et al.(1989) PNAS USA 86:6176-6180.

W-PM-B1

Kinetic Studies of Interprotein Electron Transfer Mechanisms. Gordon Tollin, James T. Hazzard, and Mark C. Walker. Department of Biochemistry, University of Arizona, Tucson, Arizona 85721.

Transient state experiments utilizing laser flash photolysis are being used to investigate the kinetics and mechanism of interprotein electron transfer in various redox proteins, including cytochrome c-cytochrome c peroxidase (CCP), ferredoxin-ferredoxin $NADP^+$ reductase and cytochrome c-cytochrome c oxidase. In all these cases, direct measurement of the kinetics of the physiologically-relevant one-electron transfer reaction within transient or stabilized protein-protein complexes can be made under a variety of conditions. These experiments have shown that, for some systems, the electrostatically most stable complex is not optimized for electron transfer, whereas for others it is. For the reduction of Compound I of CCP by reduced cytochrome c, studies with several site-specific mutants show that the Poulos-Kraut model is probably incorrect, at least in some aspects, and have raised interesting new questions concerning the role of specific amino acid side chains in the electron transfer process. Work supported by NIH grant DK15057.

W-PM-B2

TOWARD UNDERSTANDING THE FUNCTIONAL PROPERTIES OF CYTOCHROME C OXIDASE SUBUNITS BY ANALYSIS OF MAMMALIAN, PLANT AND BACTERIAL ENZYMES. S. Ferguson-Miller, Biochemistry Dept., Michigan State University, E. Lansing, MI 48824

The individual roles of the subunits of cytochrome c oxidase are not known. Studies on the mammalian enzyme depleted of subunit III indicate that this peptide contributes to enzyme stability but is not essential for proton pumping or other measureable functions. Yet we find a subunit III-like peptide in R. sphaeroides aa_3-oxidase, emphasizing its high degree of conservation. Studies on mammalian subunit II, cloned and expressed in Xenopus oocytes and in vitro show that a native-like, membrane-bound peptide is produced, indicating the potential of this approach for determining individual subunit characteristics. Important clues to subunit function are also derived from the study of plant cytochrome oxidases which show: unique spectral characteristics related to an altered heme a environment; 3-4 small peptides with no size or antigenic similarly to yeast or mammalian subunits; a different (developmental?) subunit in wheat germ; and a role for subunit IV in cytochrome c binding affinity. Supported by NIH Grant GM26916.

W-PM-B3

PRIMARY INTERMEDIATES IN THE REACTION OF CYTOCHROME *C* OXIDASE WITH OXYGEN

Sanghwa Han, Yuan-chin Ching, and Denis L. Rousseau

AT&T Bell Laboratories, Murray Hill, NJ 07974

The primary intermediates in the reaction of oxygen with fully reduced and mixed valence cytochrome *c* oxidase were generated in a rapid mixing continuous flow apparatus. In the primary intermediate of both forms of the enzyme the $Fe–O_2$ stretching mode is located at 568 cm^{-1} and its assignment was confirmed by oxygen isotope studies. These data demonstrate that: 1. The primary intermediate in the reaction of oxygen with fully reduced cytochrome *c* oxidase may be generated at room temperature; 2. The oxidation state of cytochrome *a* plays no role in the structure of the oxygen binding site; 3. The initial $Fe–O_2$ bonding does not have any unique structural features which could lead to the rapid reduction of dioxygen to water.

W-PM-B4

Effects of incorporation into liposomes on components of quinol cytochrome c reductase J.C. Salerno, M. Osgood, C.H. Kim, and B. Daro Biology Dept. and Center for Biochem. and Biophys., RPI, Troy, N.Y. 12180 (supported by NIH GM 34306)
Phospholipids have long been known to be an essential component of many integral membrane enzyme complexes. Lipid depletion converts the b cytochromes of QCR to denatured 5 and 6 coordinate forms by optical and epr criteria. Reconstitution into proteoliposomes restores most of even the five coordinate form to the native state. Reference to current molecular models suggests that secondary structural changes are involved. In intact QCR, the epr spectrum of the Rieske Fe/S center is sensitive to the redox state of quinone. In lipid depleted QCR, the center assumes a spectroscopically distinct state which is Q insensitive. Reconstitution into liposomes restores both the native state and Q sensitivity. Loss of the ability of center o to bind Q appears to be the cause of inactivation in lipid depleted QCR.

Differential tendency to incorporate allows membrane protein complexes and fractions to be separated during reconstitution with limiting PL. Cytochrome c_1 can also be renatured by reconstitution.

W-PM-B5

STUDIES ON THE MECHANISM AND POSITION OF THE Q_O SITE OF UBIQUINOL CYT c_2 OXIDOREDUCTASE (CYT bc_1)

D. E. Robertson, *F. Daldal & P. L. Dutton. Depts. of Biochemistry & Biophysics &*Biology, Univ. of Pennsylvania, Philadelphia, PA, 19104

In the absence of three-dimensional structural information, questions remain regarding the site positions, amino acid determinants and mechanisms of redox catalysis at the two ubiquinone sites of cyt *bc*. We have addressed these problems in *Rhodobacter capsulatus* using Ps+ mutants selected for resistance to Q_o site specific inhibitors. In the majority of mutants selected for resistance to myxothiazol, mucidin or stigmatellin, a total of six residues in the cyt *b* polypeptide are substituted to acheive the phenotypes. Five of these residues are near the outer edge of the cytoplasmic membrane in accord with carotenoid bandshift data implying that Qo is near the edge of the low dielectric medium (Robertson, *et al* (1989) *Biochim. Biopys. Acta* 935, 273) Mutants selected for myxothiazol or mucidin resistance show alterations in the rates of ubiquinol oxidation via site Q_o while those selected for stigmatellin resistance differ little from wild-type. A single mutant substituting proline for leucine near the center of the membrane has a slight effect on Qi function. One mutant cross-resistant to stigmatellin exhibits a lowered affinity for Q as demonstated by the 2Fe2S EPR lineshape. The effects of substitutions on rate limitation and the use of these mutants to predict amino acid determinants of Q_o and Q_i will be discussed.

Supported by PHS Grants GM27309 and GM38237.

W-PM-B7

PROTON PUMPING IN CYTOCHROME C OXIDASE.

Sunney I. Chan, Noyes Laboratory of Chemical Physics, 127-72, California Institute of Technology, Pasadena, CA 91125

The basic requirements for a redox-linked proton pump will be discussed. Several mechanistic models of redox linkage that attempt to build in these requirements at the molecular level will be presented for cytochrome c oxidase. The extent to which each model embodies these principles and offers predictions that match the experimental facts will be reviewed.

W-PM-B6

ASSEMBLY AND STRUCTURE OF COMPLEX I

H. Weiss, University Düsseldorf, FRG

We found that in mitochondria of N. crassa a small, rotenone-insensitive form of complex I is made when mitochondrial protein synthesis is inhibited. This small complex contains only subunits which are homologuous to nuclear encoded subunits of the large complex, and as redox centres FMN and the Fe-S clusters N-1, N-3 and N-4. The small complex is devoid of mitochondrially encoded subunits and cluster N-2. We studied the pathway on which the large complex I is assembled and identified an intermediate which contains all mitochondrially encoded subunits and only such nuclear encoded subunits which are not found in the small complex. This result suggests that complex I emerged from two preexisting electron transfer complexes of which one contributed the electron input part and the other the electron output part of complex I.

Friedrich, T. et al. (1989) Eur. J. Biochem. 180, 173-180

W-PM-C1

ION CHANNEL SUBCONDUCTANCE STATES

James A. Fox, Neurex Corporation, 3760 Haven Avenue, Menlo Park, CA 94025.

Open ion channels may have more than one conductance state. Subconductance states have been reported for a wide variety of ion channels, and have been studied in intact tissue, cultured cells, cell lines, and reconstituted systems. Study of subconductance states may provide important information about channel structure and gating not available from study of the main conductance state alone. For example, multiple substates of equal conductance suggest a subunit structure of the channel, and the existence of a mechanism for cooperative gating of the subunits. Substates with unequal conductances suggest that the channel molecule may have more than one stable conformation, or that ions or blockers have bound to the channel. Regulation of channel conductance may be an important aspect of cellular physiology.

W-PM-C2

EFFECTS OF INTERNAL Mg^{2+} ON FAST K CHANNELS IN MOLLUSCAN NEURONES

V.N.Kazachenko, V.I.Geletyuk, E.V.Fomina

Institute of Biological Physics of the USSR Academy of Sciences, Pushchino, Moscow Region, 142292, USSR

Using the patch-clamp method single K^+channels of different conductance, from 5 to 30 pS (at internal and external K^+ concentrations of 100 and 1.5 mM, respectively, and V = 0) were studied. The channels were identified as subtypes of the fast potential-dependent K^+ channel (probably A-channel). Effects of internal Mg^{2+} on the channel conductance and the channel kinetic behaviour were examined. It was found that Mg^{2+} inhibits the channel conductance (g) and modifies the channel kinetics (decreases the probability of the channel open state). An apparent blocking constant (K_B) for the channel conductance is a potential-independent parameter related to the subtype channel conductance (g) by an approximate relation: $K_B = a + bg^3$ (a and b are constants). The channels subtypes are regarded as conductance oligomers of different order composed of various numbers of identical conductance monomers.

W-PM-C3

KINASE- AND TEMPERATURE-REGULATED CHLORIDE CHANNELS IN NORMAL HUMAN T LYMPHOCYTES.

P.A. Pahapill and L.C. Schlichter. Dept. of Physiology, University of Toronto, Toronto, Canada. M5S 1A8.

Maxi-chloride channels (200-400 pS) have been seen in several cell types, but usually only in exised patches and at unphysiological voltages (ie. +/- 20 mV); conditions that make their physiological relevance questionable. We have characterized maxi-chloride channels in normal human T lymphocytes (Schlichter et.al., in press) and have now found conditions that activate them at the resting potential. In exised patches, maxi-chloride channels are activated by the catalytic subunit of PKA plus ATP (1 mM). In cell-attached patches, activation occurs at 37°C at rest and increases with hyperpolariztion; ie. the voltage dependence is altered. Channel activation appears as increased co-operativity of many small "co-channels" resulting in a co-ordinated maxi-chloride channel with several sub-conductance states. These results emphasize the importance of making cell-attached recordings at normal physiological temperatures. Supported by MRC and NCIC (Canada).

W-PM-C4

CONDITIONS THAT INFLUENCE THE OPEN TIME HISTOGRAMS OF SODIUM CHANNELS

K. Nagy, Institut für Biologie II, RWTH, Kopernikusstr. 16, D 5100 Aachen, FRG

Single sodium channel currents were recorded in neuroblastoma cells in cell-attached configurations at 10°C. Open time histograms constructed under different conditions could be best fitted by multiexponential functions. The fits` time constants: 1) were dependent on the prepulse potential, 2) showed time histograms depended on whether previous openings had occured. Results indicate that the number of open states is higher then estimated from the fits. In which state the channel opens depends on several conditions. The gating of channels may be non-independent. After inhibition of inactivation by toxin subconductance states were observed suggesting substates for the native channels. Sodium channels may have some discrete open states and probably several conformational substates with different life times and unitary conductance.

W-PM-C5

THE EFFECT OF pH ON SUBCONDUCTANCE STATE FREQUENCY AND DURATION IN BURSTING Na+ CHANNELS OF SKELETAL MUSCLE.

Joseph Patlak, Dept. of Physiology, U. of Vermont, Burlington, VT 05405.

Na^+ channels of mouse skeletal muscle enter one or more subconductance levels, both under normal recording conditions, as well as with DPI-201-106 present to induce prolonged bursting activity. The most common sublevel is about 35-40% of the amplitude of the fully open level, but individual events can have amplitudes between 10-50% and about 80% of the fully open level. With physiological saline in the patch pipette (pH 7.4), and 130 mM CsAspartate buffered to pH 7.4 on the cytoplasmic side of the patch, sublevels comprise about 2-6% of the total open time of a bursting Na^+ channel. The lifetime of the sublevel events is usually significantly shorter than that of the full state. When the pH of the solution on the cytoplasmic side is decreased to values below 6.0, the proportion of time spent in sublevels increased to as much as 20%, with little or no increase in the variance of the fully open level. The increase in sublevels is due to their increased frequency, without large changes in the lifetime of either the sublevel or the fully open states. The alteration of sublevel occupancy is relatively slow (minutes) following change in pH, and it is reversible. Sublevel frequency is relatively insensitive to other components of the bathing solutions. I speculate that the sublevel events are due to alterations in the tertiary structure of the channel molecule that are promoted by acidic conditions on the channel's cytoplasmic side. Supported by NIH AR37606. The author is an Established Investigator of the AHA.

W-PM-C6

SUBSTATE ANALYSIS OF THE CARDIAC SODIUM CHANNEL

Wolfgang Schreibmayer, Institute for Medical Physics and Biophysics, Harrachgasse 21/IV, A-8010 Graz, Austria

Conductance substates of the cardiac sodium channel (csc, rat ventricular cells) were induced by using different modifiers of gating behaviour, namly S-DPI 201-106 (s), toxin-II form anemonia sulcata (a), veratridine (v), Brevetoxin-3 (b) and mixtures of these agents. Current ratios (cr), slope conductances, reversal potentials and saturation characteristics were evaluated for the individual channel substates.

The results were as follows: (i) Cr's fell into a pattern of six equidistant values (I-VI) irrespective of ionic strength and the modifying agents (a, b, s, v) applied (corresponding cr values read 0.20, 0.34, 0.51, 0.69, 0.85 and 1.00, respectively). The slope conductances could be determined for the individual substates and are also consistent with six open substates which are integer multiples of the conductance of state I. (ii) The permeability ratio $P_{Na}{}^+/P_K{}^+$ (measured as the reversal potential of substate currents) of the csc was conserved both for the different gating modifiers used and for the different substates. (iii) Saturation analysis revealed that subconducting states II and VI have different maximal conductances ($ge_{VImax} = 2.9 \times ge_{IImax}$) but identical apparent affinities for sodium ($K_{NaVI} = 286$ mM; $K_{NaII} = 303$ mM).

These findings seriously challenge the conception that rectangular current events of the csc normally observed with the patch clamp methods reflect ion passage through only one single ion pathway. Alternatively, the view that instead 6 or 3 pores with synchronized gating ("oligochannel") underly these rectangular current events can account readily for the observed properties of the substates and does not contradict to any known properties of "the" csc. In addition this postulated quarternary structure of the csc protein entails dramatic consequences for our understanding of the voltage dependent gating process and on the interpretation of drug and toxin action on the csc.

This work was supported by the Austrian Research Foundation (S45).

W-PM-C7

EXPERIMENTAL STRATEGIES TO INVESTIGATE THE STRUCTURAL BASIS OF REGULAR SUBCONDUCTANCE PATTERNS OBSERVED FOR SEVERAL ION CHANNELS

H.Schindler, Institute for Biophysics, University of Linz, 4040 Linz/Auhof, Austria

Single conductance events of a variety of ion channels show regular sublevel patterns which are not readily explained by substates of a single ion pathway ("monochannel") but may well reflect the synchronized activity of several pores in a channel protein associate ("oligochannel"). Conclusive decisions in this conceptual dilemma is not expected from patch clamp studies alone. For this, we have devised experimental strategies which are presented: (i) planar membrane reconstitution under control of the lateral distribution of channel proteins (ii) FPC (Fluorescent Particle Counting) which allows to quantitate and follow in time the association state of channel proteins down to dimerization at typical membrane channel densities. These techniques, combined with electron microscopy and x-ray crystallography have brought conclusive evidence that omp F porin (matrix protein of E.coli outer membrane) forms oligochannels. Application of this strategy to other channels now provided evidences, although still less conclusive compared with porin, that several of these channels represent "oligochannels" as well, which will be summarized.

W-PM-C8

POSITIVE COOPERATIVITY AS A DETERMINANT OF GATING PROPERTIES AND VOLTAGE SENSITIVITY OF SKELETAL MUSCLE CALCIUM CHANNELS.

Lin Hymel and Hansgeorg Schindler, Inst. for Biophysics, Univ. of Linz, Austria; Hartmut Glossmann, Inst. for Biochem. Pharmacol., Innsbruck, Austria; and Sidney Fleischer, Dept. Mol. Biol., Vanderbilt Univ., Nashville, TN.

The purified L-type and Ca^{2+}-release channels (CRC) have been characterized using the septum-supported, vesicle-derived planar bilayer method (SVB). SVB allows incorporation of a predetermined density of purified channel proteins whose interactions can be inferred from changes in functional properties with time. For the L-type channel, we observe conductance levels both smaller and larger than the native conductance of 12 pS. Initially, overlapping smaller events (1 pS from fluctuation analysis) are observed whose opening probability (P_o) is independent of voltage. After a few minutes, however, discrete events of up to 60 pS are observed whose P_o increases nonlinearly at voltages from 0 to +100 mV at the protein side, mimicking the voltage dependence (VDep) of the native channel. This transition to a VDep channel appears to involve diffusion-controlled channel protein association, which occurs faster if a higher initial channel density is used. The CRC, which is a tetrameric complex (foot structure), shows Vdep from the outset, also activating predominantly at positive potentials. Statistical analysis indicates synchronization of oligomeric structures for both channels. These results constitute strong evidence for positive cooperativity in controlling the gating and in particular the VDep of calcium channels and their possible interactions in the triad junction. [NIH DK 14632 for SF]

W-PM-C9

THE DHP-SENSITIVE CALCIUM CHANNEL IN GH_3 CELLS EXHIBITS MULTIPLE CONDUCTANCE LEVELS. D.L. Kunze & A.K. Ritchie*. Dept. Molecular Physiology and Biophysics, Baylor College of Medicine, Houston, TX 77030 and *Dept. Physiology and Biophysics, Univ. of Texas Medical Branch, Galveston, TX 77550. Calcium channels in the GH_3 anterior pituitary cell line exhibit at least five conductance levels when examined in cell-attached patches (pipette (in mM): 100 $BaCl_2$, 10 Hepes; bath: 140 KAsp, 10 Hepes, 10 EGTA, 1 $MgCl_2$) or outside-out patches (pipette: 105 NMDG Asp, 15 EGTA, 5 BAPTA, 10 Hepes, 2.5 $MgCl_2$ or 124 CsCl, 11 EGTA, 1 $CaCl_2$, 2 $MgCl_2$, 10 Hepes; bath: 100 $BaCl_2$, 10 Hepes). These channels are reversibly inhibited by the dihydropyridine (DHP) calcium channel antagonist nimodipine (10^{-7}M) and activated by the DHP agonist BAY K 8644 (10^{-7}M). Mean open times for the five conductance levels were brief (<1 ms) in control solutions but increased in the presence of BAY K 8644. In 100 mM external Ba^{2+} and BAY K 8644, slope conductances of approximately 8-9, 12-13, 16-18, 23-24, and 28 pS were calculated from single channel analyses over a voltage range of -30 to 0 mV. During attempts to manipulate conductance levels by altering the contents of the pipette solution multiple levels were observed in outside-out patches in the presence or absence of ATP, cAMP and/or GTP. The occurrence of multiple conductance levels for DHP-sensitive Ca^{2+} channels has been reported for calcium channels that have been reconstituted into lipid bilayers. The present study indicates that the frequent occurrence of multiple conductance states of the Ca^{2+} channel exists in native membranes and is thus not unique to reconstituted channels. The presence of multiple conductance states may explain the wide range of unitary conductances (7 to 28 pS) that have been reported for this channel in GH_3 cells. Supported by NIH NS23573 (DLK) and DK33898 (AKR).

W-PM-C10

COOPERATIVITY OF L-TYPE CA CHANNELS DURING THE INACTIVATION PROCESS.

M. Mazzanti and L. J. DeFelice.

Dept. of Anatomy and Cell Biology, Emory University, Atlanta GA 30322.

We investigate the voltage and time dependency of L-type Ca channels using patch-clamp technique on 7-day embryonic chick ventricle cells. With 20 mM Ba as charge carrier in cell-attached configuration, we recorded single channel activity in 50% of the experiments. Delivering voltage steps from a holding potential of -80 mV to -20,-10, 0,+10 and +20 mV membrane potential decreases single channels amplitude, but, at the same time, increases the mean open time of the channel at more depolarized potentials.
When the patch of membrane contains several channels the average current shows inactivation over a step of 500 msec. Offsetting the holding potential from -80 mV to -40 mV reduces the average current while the inactivation time constant greatly increases. Histogram analysis of the records at depolarized holding potentials shows a decrement of the number of active Ca channels in the patch, and no change in the single channel amplitude. (Supported by NIH PO1 HL27385 09A1).

W-PM-C11

ION CHANNEL PERMEATION MECHANISMS: THE PROBLEM OF CONDUCTANCE SUBSTATES.

John A. Dani. Dept. of Molecular Physiology & Biophysics, Baylor College of Medicine, Houston TX 77030

Various permeation models will be briefly summarized. Eyring rate theory and continuum approaches based on the Nernst-Planck differential equation have long provided quantitative methods for analyzing and describing ion permeation. Recently, more sophisticated models have been used to account for physical properties of channels. Continuum and rate theory models or the combination of the two have accounted for gross structural features of channels and for ionic interactions within channels. Molecular motions have been modeled to influence ion transport via time-dependent fluctuations in the energy profile.

The discussion will explore whether classic ion permeation mechanisms can provide a formalism to account for regular substate patterns. Possibly, staircase-like transitions in the single-channel current record are caused by conformational changes of one channel. Structural mechanisms of the channel will be examined. The question is the following: can a single channel produce a pattern of regular conductance substates or must there be synchronized gating of many channels? Supported by MDA, Whitaker Foundation and NIH NS21229.

W-PM-D1

THE STRUCTURE OF THE ACTIN-DNASE I COMPLEX AT 3.0 Å RESOLUTION AND THE DERIVED STRUCTURE OF F-ACTIN. W.Kabsch and K.C. Holmes. Max Planck Institut fur medizinische Forschung Heidelberg, FRG

The structure of the complex between rabbit skeletal muscle actin and bovine pancreatic DNase I has been solved at 3 Å resolution by x-ray crystallography. The atomic model of actin was derived by combining phase information from two heavy atoms to 4 Å resolution with the known atomic structure of DNase I. Using two global temp. factors and all data, an R factor of 23.5% has been achieved. Actin consists of two domains with a cleft in between. Each domain consists of two domains. Subdomains 1 and 2 constitute the smaller domain and 3 and 4 the larger. Subdomain 1 contains both C and N termini and a 5-stranded β-sheet surrounded by 5 helices. The β-sheet comprises a β meander and a β-α-β unit. Subdomain 2, which is inserted into 1, consists of a 3-stranded antiparallel β-sheet with a helix connecting the two edge strands. Part of the loop between the first and second strand is incorporated as an edge strand in a β-sheet of DNase I, probably distorting the actin structure. Subdomain 3 consists of a β sheet with the same possible topology as subdomain 1, indicating that gene duplication. At the C-terminal end of 3 the polypeptide crosses over the cleft

Continued on Next Abstract

W-PM-D1—Continued

to subdomain 1 which also contains the C terminus.Sub-domain 4, which is inserted into 3, consists of a two stranded anti-parallel β sheet and four helices. The last of these helices is contiguous to and aligned with a helix in domain 3 to form a broken helix about 40 Å long. The two are connected by a loop which sticks out into the inter-molecular space. ADP is bound between the large and small domains S14, G15, and K18 of subdomain 1 and D157 and G302 of sub-domains 3 form hydrogen bonds with the diphosphate. The ribose is bound to D157 and E214. The adenine nucleotide fits into a pocket formed by K213, T303, and Y306. A Ca ion is bound to the (β-phosphate) and to D154, Q137, and D11. The rigor myosin binding site is on the N-terminal surface of subdomain 1 from cross-linking studies. The atomic coordinates and the observed diffraction from orientated actin have been used to find the best actin monomer orientation in the fibre. A unique best fit puts the large domain on the inside (nearest to the helix axis) with the long axis of the large domain approximately along the two start long actin helix. The long broken helix is parallel to the axis and contacts the symm etry-related long broken helix across the axis. The small domain is at large radius and does not appear to be involved in helix contacts. The myosin site is at large radius and agrees with the position derived from E.M.

W-PM-D2

THE EFFECT OF CALCIUM ON THE PHOSPHATE RELEASE STEP OF THE ACTOMYOSIN ATPASE IN SKINNED PSOAS MUSCLE FIBERS.

N. Millar, J. Lacktis & E. Homsher. Dept. of Physiology, UCLA School of Medicine, Los Angeles, CA 90024.

Calcium is thought to control muscle contraction by regulation of a step in the crossbridge cycle that follows weak attachment but precedes force development and product release, since at low ionic strength low [Ca] inhibits the actoS1 ATPase without inhibiting association, and in fibers at low [Ca] crossbridges can attach without generating force (Brenner, Ann. Rev. Physiol, 42, 655, 1987). The force generating step is closely coupled to phosphate release, and photogeneration of phosphate in an isometrically contracting fiber causes an exponential decline in tension, the "Pi transient" (Dantzig et al, Biophys J, 51, 3a, 1987). The dependence of the Pi transient rate constant on Pi concentration reveals that Pi release is a 2 step process: an isomerization of an A.M.ADP.Pi state (the force producing step), followed by Pi release. It has previously been shown that the rate of the Pi transient is not affected by reducing [Ca] from pCa 4.5 to 6.5 (Homsher & Lacktis, Biophys J, 55, 261a, 1989), but experiments at very low activations (<20% P_0) in the presence of Pi show that both the rate constant and relative amplitude of the Pi transient increase compared to those at full activation. At 1mM Pi (10°C) reducing [Ca] from pCa 4.5 to 7.0 has no effect on the rate of the Pi transient ($40s^{-1}$), but increases the amplitude by 30%, while at 5mM Pi both the rate and amplitude are approximately doubled from $55s^{-1}$, 5% to $110s^{-1}$, 8%. These data indicate that Ca does not directly regulate the Pi release step itself, but one prior to Pi release, possibly the force-generating isomerization. (Supported by NIH grant AM30988-08).

W-PM-D3

CALDESMON INHIBITS GENERATION OF ACTIVE TENSION IN SKINNED RABBIT PSOAS FIBERS BY BLOCKING ATTACHMENT OF WEAK BINDING CROSS-BRIDGES TO ACTIN. B. Brenner*, L.C. Yu~, and J.M. Chalovich#; *University of ULM, FRG; ~NIH and #E. Carolina Univ. Caldesmon (or its actin-binding fragment) reversibly reduces the stiffness of relaxed fibers and simultaneously changes the equatorial X-ray reflections. This indicates a reduction in the number of crossbridges weakly bound to actin. In rigor or with MgPPi (strong binding states) stiffness and equatorial reflections are unaffected. Furthermore, active tension (pCa 4.5) is reduced both at low and physiological ionic strengths while crossbridge turnover kinetics (rate constant of force redevelopment) are unaffected. These data demonstrate that (a) attachment, albeit transient, of a weak binding state is essential for force generation (active crossbridge turnover); (b) caldesmon inhibits force generation by a steric blocking mechanism (blocking of crossbridge attachment prior to the force generation without effecting crossbridge turnover kinetics). This is in sharp contrast to the troponin-tropomyosin system in which turnover kinetics but not crossbridge attachment is regulated (Chalovich et al. 1981; Brenner, 1988).

W-PM-D4

ORIENTATION OF RHODAMINE BOUND TO SH-1 ON THE MYOSIN HEAD REPORTS NUCLEOTIDE BINDING RATHER THAN THE CROSS-BRIDGE POWER STROKE.

J.W. Tanner, D.D. Thomas+, & Y.E. Goldman. U. of PA Dept. Physio., Phila., PA, 19104 & U. of MN Dept. Biochem.+, Mpls., MN, 55455.

Are motions of iodoacetamidotetramethyl rhodamine probes, covalently bound to SH-1 (Cys-707 of myosin heavy chain), related to development of force? We monitored tension and probe absorption dichroism in single glycerol-extracted rabbit psoas muscle fibers during activation from rigor by photolysis of caged ATP in the presence of ~30 μM Ca^{2+} (setup: Tanner et al., Biophys. J. 55:9a, 1989). Dichroism is negative in rigor (indicating average probe angle > 54.7° from the fiber axis) and positive (angle < 54.7°) in rigor plus 4 mM ADP or during active contraction (Burghardt et al., PNAS 80:7515, 1983). Dichroism reversed sign within 30 ms after photorelease of 1 mM ATP (figure, arrow), but changed only slightly during tension development. In chart recordings during the onset of rigor from relaxation, force generation preceded the change in dichroism. In both cases, the probe motions were temporally separated from the power stroke, but correlated with nucleotide binding or release.

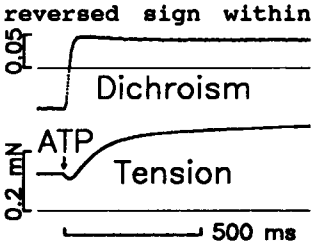

Supported by the MDA & NIH grants AR26846 & AR32961.

W-PM-D5

SPECIFICITY AND ORIENTATION OF IODOACETAMIDO PROXYL SPIN LABELED MYOSIN SUBFRAGMENT 1 DECORATING MUSCLE FIBERS.

K. Ajtai, L. Poto and T. P. Burghardt, Dept. Biochem. & Molec. Biol., Mayo Foundation, Rochester, MN 55905

The nitroxide spin label iodoacetamido PROXYL (IPSL) was specifically and rigidly attached to sulfhydryl 1 (SH1) on myosin subfragment 1 (S1). The specificity of this label for SH1 was demonstrated using a new technique wherein spin label is localized on the electrophoresis-isolated proteolytic fragments of myosin using electron spin resonance (ESR). Studies of the rigidity of the probe on SH1 indicate that the IPSL is immobilized on the surface of S1 in the presence and absence of the nucleotides MgADP or MgATP. The ESR spectrum of muscle fibers decorated with IPSL-S1 shows that the IPSL-S1 rotates upon binding MgADP. The angular displacement due to nucleotide binding is larger than that detected with the maleimido TEMPO spin label demonstrating that the IPSL is oriented on the myosin cross-bridge in a manner that is favorable for detecting cross-bridge rotation.

Funding was from NSF grant DMB-8819755 and Mayo Foundation. TPB is an Established Investigator of the AHA.

W-PM-D6

CROSSBRIDGE STRAIGHTENING TO GENERATE FORCE

by S. Highsmith and D. Eden (UOP and SFSU)

The rotational correlation coefficient ,τ, was measured for myosin subfragment-1 (S1) in the presense of MgADP and MgADP•V by using transient electrical birefringence methods. The removal of V increases τ from 244±10 to 267±6 ns. This result confirms the conclusion of Aguirre etal (1989 Bioch 28, 799) that V binding to S1•MgADP increases its rate of rotational Brownian motion, but our data are correlated quantitatively with S1 size. The change in τ for S1•MgADP•V going to S1•MgADP is consistent with S1 becoming less flexible or less symmetrical in solution at 3°C.

This result can be interpreted as a change in the bend-angle of a rigid S1 that can bend at its center (Garcia de la Torré & Bloomfield 1982 Quart. Rev. Biophys. 14, 81). The observed increase in τ is consistent with one segment of a rigid bent S1•MgADP•V rotating 32° to produce a rigid straight S1•MgADP as V dissociates. If S1 has a straight length of 19 nm, the tip of the rotating segment moves 5.2 nm, enough for a power stroke. This model suggests force generation in muscle can be due to bound bent S1•MgADP•P straightening out as P_i dissociates, its tip traversing 5.2 nm with actin bound. (AR37499 and GM31674)

W-PM-D7

ENERGETICS AND STOCHASTIC STRUCTURE OF IN-VITRO MICROTUBULE MOVEMENT.

F. Gittes*, A.G. Moss, G.B. Witman and P. Verdugo*. Worcester Foundation for Experimental Biology, Shrewsbury, MA 01545, and *Center for Bioengineering, University of Washington, Seattle, WA 98195.

Glass-bound dynein can induce ATP-dependent microtubule (MT) translocation. When motion is sufficently resolved in time and space, the monotonic one-directional MT movement is found to be an average over forward and backward motions that are apparently random. The present studies investigate whether the random elements of MT movement correspond to passive Brownian motion or whether, alternatively, they reflect a characteristic feature of dynein-ATP-driven MT translation. Experiments were conducted using β/IC1-subunit dynein as the motor molecule. Transport was observed in MTs of different lengths at low and high ATP concenrations, and also in preparations exposed to vanadate.

The results in all cases show that MTs spend a large fraction of time immobile. Movement, when it occurs, takes place in fast, discrete and random jumps which last less than 1 msec. These jumps are bidirectional and can reach up to 1 μm in length. Calculations of energy dissipation show that these discrete motions cannot be driven by thermal fluctuation. Hence they must be powered by ATP hydrolysis, and probably reveal a characteristic property of the underlying dynein-MT interaction that generates mechanical work in this system. These observations indicate that the random features of MT translocation cannot be explained by passive thermal Brownian motion.

Supported by grants GM 30626, HD 23858, CA 12708 from NIH to G.B.W. and HL 38494 from NIH and R 010 7 01 from the CFF to P.V.

W-PM-D8

FORCE OF KINESIN-DEPENDENT MICROTUBULE TRANSLOCATION MEASURED BY OPTICAL TRAPPING.

Scot C. Kuo and Michael P. Sheetz
Department of Cell Biology & Physiology
Washington University Medical School
Saint Louis, MO 63110

Using limiting dilutions of squid kinesin adsorbed to a microscope slide in the presence of carrier protein, microtubules can be translocated by a single attachment point, presumably by a single kinesin molecule (Howard *et al.*, 1989, *Biophys J 55*, 193a). We have attached latex beads to translocating microtubules, and can stop the movement of these microtubules by a single-beam optical trap. The optical trap uses radiation pressure of near-infrared laser illumination to trap microscopic particles (Ashkin *et al.*, 1987, *Science 235*, 1517; *Nature 330*, 769). The force of the optical trap was calibrated by viscous drag on latex beads. The force of a single kinesin attachment site is less than 6 piconewtons. The same experimental configuration can also provide a force-velocity measurement of kinesin, which we are currently pursuing. A videotape demonstrating the technique will be shown.

W-PM-E1

Ruminations on the Mechanism of Ca^{2+} induced Ca^{2+} Release, M. Morad, Dept. of Physiology, Univ. of Penn., Philadelphia, PA.

In cardiac muscle the release of Ca^{2+} from the SR is regulated by the Ca^{2+} channel. The Ca^{2+} induced Ca^{2+} release hypothesis best fits the experimental findings, and supposes that: a) Ca^{2+} binding to a receptor site opens the release channel, & b) prolonged presence of Ca^{2+} at the site inactivates the channel. Data in support of this hypothesis comes from: 1) similarity in the voltage-dependence of Ca_i^{2+} transients, contraction and the I_{Ca}; 2) Ca^{2+} release is activated by influx of Ca^{2+} but not Na^+ or Ba^{2+} through the Ca^{2+} channel; 3) small elevation of $(Ca^{2+})_i$ releases the SR Ca^{2+} in skinned, or intact cardiac myocytes; 4) Ca^{2+} directly activates the release channel in isolated vessicles or single channels incorporated in bilayers. The inactivation of Ca^{2+} release channels is less well understood, but is a mandatory step if the Ca^{2+} induced release mechanism is to be graded. The evidence in support of this hypothesis is that slow elevation of $(Ca^{2+})_i$ in skinned myocytes suppresses the Ca^{2+} release. Rapid photolytic release of Ca^{2+} from DM nitrophen in intact myocytes, either at onset or during the I_{Ca}-gated release, however, failed to terminate Ca^{2+} release. In this respect, Ca^{2+} release channels fail to show significant inacativation when exposed to higher Ca^{2+} concentrations. The inherent difficulty of the Ca^{2+} induced Ca^{2+} release hypothesis is the mechanism by which the Ca^{2+} receptor site distinguishes between the alternate roles of Ca^{2+} channel Ca^{2+} and the SR Ca^{2+} in the activation and inactivation of the release mechanism. These considerations do not invalidate the Ca^{2+} induced inactivation hypothesis, but they do point to its limitations. Alternative models and mechanisms will be discussed in light of newer experimental findings.

W-PM-E3

REGULATION OF SARCOPLASMIC RETICULUM CA^{2+} RELEASE CHANNEL ACTIVITY. L. Xu, K. Anderson and G. Meissner. Dept. of Biochemistry, Univ. of North Carolina, Chapel Hill, NC 27599-7260.

Regulation of sarcoplasmic reticulum Ca^{2+} release channel activity by T-tubule membrane potentials and the channel-activating ligand Ca^{2+} was examined by studying the $^{45}Ca^{2+}$ release behavior of junctional T-tubule/sarcoplasmic reticulum (SR) complexes ("triads") and by reconstituting the purified 30S release channel complex into planar bilayers. T-tubule depolarization induced $^{45}Ca^{2+}$ release from the SR compartments of triads that was inhibited by the two Ca^{2+} release channel blockers Mg^{2+} and ruthenium red as well as by the T-tubule DHP receptor ligand, nifedipine. Single channel measurements with the K^+-conducting (750pS in 0.25M K^+) release channel revealed that channel activity is, as previously reported, regulated by cis (cytoplasmic) Ca^{2+}. Open probability, open and closed lifetimes, and Ca^{2+}-dependence of the Ca^{2+}-gated channel were modified by trans (SR luminal) Ca^{2+} and cis Mg-ATP. Trans Ca^{2+} shifted E_{rev} to more positive values and reduced K^+ conductance at negative and positive voltages. Supported by NIH.

W-PM-E2

CALCIUM TRANSIENTS IN RAT SKELETAL MUSCLE: EVIDENCE FOR A Ca^{2+}-REGULATED Ca^{2+} RELEASE PROCESS. J. García & E Stefani. Dept. Molecular Physiology & Biophysics, Baylor College of Medicine, Houston, TX, 77030.

Calcium transients were recorded in single rat skeletal fibers dissected from e.d.l. muscles using the Vaseline gap voltage clamp technique. The only permeable ion in the extracellular solution was Ca^{2+} (2 mM). The intracellular solution contained the Ca^{2+} indicator Antipyrylazo III (1 mM) and EGTA (0.1 mM). Calcium transients had a detection threshold at -50 mV, and reached a maximum $[Ca^{2+}]$ of about 10 μM for membrane potentials from 0 to +100 mV. After the termination of pulses (100-200 ms) to -10-+50 mV, the transients kept increasing for several milliseconds and then slowly decayed to the resting level. The model of Brum et al. (1988, J. Physiol., 398) was used to calculate the Ca^{2+} release from the SR. It was first fitted to the smallest (-40 mV) transients to find the best parameters and thereafter to the larger transients. With this procedure, it was evident that the release process was still active after the pulses. The maximum rate of release was about 10 μM/ms. These results suggest that Ca^{2+} release from the SR may be regulated by the Ca^{2+} concentration in the myoplasm. Supported by NIH and MDA.

W-PM-E4

CONTRACTIONS OF DYSGENIC SKELETAL MUSCLE MEDIATED BY A POTENTIATED, ENDOGENOUS CALCIUM CURRENT. Brett Adams and Kurt Beam, Department of Physiology, Colorado State University, Fort Collins, CO, 80523.

Skeletal muscle from mice with muscular dysgenesis displays an endogenous, dihydropyridine (DHP)-sensitive Ca current ($I_{Ca\text{-}dys}$). In the presence of 10 mM external Ca, $I_{Ca\text{-}dys}$ is small (-1 pA/pF) and dysgenic myotubes do not contract upon depolarization. However, following potentiation of $I_{Ca\text{-}dys}$ by 1 uM racemic Bay K 8644, some dysgenic myotubes twitch in response to direct electrical stimulation. These twitches are blocked by external Cd, by Ca removal, or by replacing Bay K 8644 with (+)-PN 200-110. Thus, unlike contractions of normal myotubes, contractions of dysgenic myotubes require Ca entry. In addition, only dysgenic myotubes having a density of potentiated $I_{Ca\text{-}dys} > -4$ pA/pF contracted, and the strength of contraction was correlated with the density of $I_{Ca\text{-}dys}$. These results indicate that the DHP receptor underlying $I_{Ca\text{-}dys}$ cannot directly couple sarcolemmal depolarization to Ca release from the SR.

Supported by grants from MDA (to KB) and from NIH (NS-24444 to KB and NS-08567 to BA).

W-PM-E5

IDENTIFICATION AND ISOLATION OF A NEW INTRINSIC JUNCTIONAL SR PROTEIN WHICH BINDS BOTH THE DIHYDROPYRIDINE AND RYANODINE RECEPTORS

A.H. Caswell, Kyungsook C. Kim, J.A. Talvenheimo and N.R. Brandt. Dept. Pharmacology, University of Miami School of Medicine, Miami, Florida 33101

The dihydropyridine receptor (DHPR) in the T-tubule and the junctional foot protein (JFP) are postulated to be the voltage sensor in the T-tubule and the SR Ca^{2+} release channel, respectively. We tested the interactions of these proteins with protein constituents in the triad junction. Electroblotted membrane vesicles were overlaid with purified [^{125}I]DHPR and [^{125}I]JFP. Neither protein probe bound to the other but both of them bound specifically to a protein of M_r of 95K present in terminal cisternae and triads but absent from T-tubules and longitudinal reticulum. It was not dissolved by either 1M KCl or Triton X100 indicating that it is intrinsic and junctional. The 95K protein was more enriched in the newly identified strong triads than the TC/triads. This protein has been isolated with app. 80% purity by two protein adsorption columns followed by molecular sieve chromatography of detergent dissolved triads. The isolated 95K protein appeared as a single major band on SDS gels. The ^{125}I protein bound to purified DHPR on spot blots. Our observations show that the DHPR interacts directly with the 95K protein, which in turn may relay the T-tubule signal to the JFP/Ca^{2+} release channel. Supported by NIH AR 21601, NIH HL39072 and MDA.

W-PM-E7

EXISTENCE OF MULTIPLE FOOT PROTEINS IN MATURE AND DEVELOPING AVIAN FAST TWITCH SKELETAL MUSCLE.

J.A. Nichol, C.F. Beck*, Y. Murakami, S. Tanksley & J.L. Sutko. Dept. Pharmacology, Univ. Nevada, Reno; *Dept. Bacteriology, Univ. Idaho.

Two polypeptides (450-500 Kd) copurify from chicken breast muscle with (^{3}H)ryanodine binding. The polypeptides differ in mol. wt., immunological cross-reactivities and peptide maps. The polypeptides are subunits of different homo-oligomeric, (^{3}H)ryanodine binding proteins, that are similar in size to the mammalian skeletal muscle foot protein. We have termed the avian muscle proteins, alpha and beta. These proteins are expressed differentially during embryonic chick skeletal muscle development. Alpha is present as early as day 12, while beta cannot be detected until between day 15 & 18. A third polypeptide, immunologically related to beta, is transiently expressed during development and may be a subunit of a third foot protein isoform. The existence of at least two differentially expressed foot proteins suggests that these proteins provide separate functions for the muscle cell. (Supported by NIH HL27470, NSF DCB8811713 and AHA).

W-PM-E6

POSITIVE FEEDBACK IN SKELETAL MUSCLE E–C COUPLING.

G. Pizarro, M. Rodríguez, L. Csernoch and E. Ríos. Rush University, Chicago, IL.

A major controversy in EC coupling regards the mechanism and role of the "hump" component $Q\gamma$ of intramembrane charge movement. Csernoch et al. (Biophys. J. 55:88a) proposed that $Q\gamma$ is the response of the voltage sensors of EC coupling to binding of Ca^{2+} to negatively charged sites on their myoplasmic face. The intracellular application of the SR channel blocker Ruthenium Red suppressed Ca release and $Q\gamma$, providing further support to the Ca binding mechanism for $Q\gamma$.

A consequence of this is the existence of positive feedback, as the movement of $Q\gamma$ should cause more openings in the release channels, in turn causing more $Q\gamma$ movement. Three experimental observations are consistent with such feedback: 1) The voltage dependence of Ca release flux has a sharp threshold at $\simeq$ –55 mV, (e–fold increase in 2 mV, Maylie et al. 1987) but does not saturate below +60 mV. 2) The fractional inactivation of the release flux during a pulse is maximum at $\simeq$ –50 mV, then decays at greater voltages and 3) the fractional inhibition of release flux by a conditioning pulse is maximum at test pulses to –50 mV. All these observations are reproduced by a model with positive feedback due to Ca binding.

W-PM-E8

INOSITOL (1,4,5) TRISPHOSPHATE (IP3) WITHIN DIAPHRAGM MUSCLE INCREASES UPON DEPOLARIZATION.

T.M. Nosek, N. Guo, J.M. Ginsburg, and R.C. Kolbeck. Dept. of Physio/Endo, Medical College of Georgia, Augusta, Ga 30912-3000

To help elucidate the role of IP3 in the control of muscle contraction, we quantified the mass of IP3 within isolated, perfused, contracting (1.5 Hz) rat diaphragms using a specific radioligand binding assay (Amersham). Muscles were rapidly frozen at various stages of the contractile cycle. We found that, immediately before stimulation, IP3 = 28 ± 3.5 pmol/mg protein (n=7) (approximately 3 μM). After stimulation and immediately before force was developed, IP3 significantly increased to 45 ± 4.5 pmol/mg protein (n=15). It remained essentially at this value for the duration of the contraction before returning to its prestimulus value.

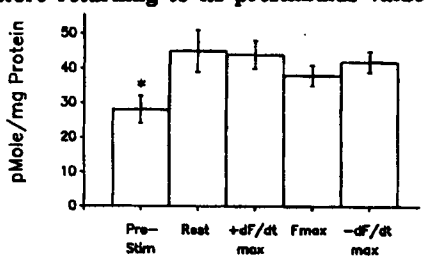

These results are consistent with the hypothesis that depolarization of the diaphragm increases phospholipase C activity and that the resultant increase in IP3 either triggers or modulates the force of the subsequent contraction. (Support: Am. Heart Assoc., GA Affil. & NIH HL/AR 37022).

W-PM-E9

METABOLISM OF INOSITOL TRISPHOSPHATE AND CALCIUM REGULATION IN SKELETAL MUSCLE. C. Hidalgo, M. A. Carrasco, R. Bull, B. Suarez-Isla and E. Jaimovich. Depto. Fisiol. Biofis., Fac. Med., U de Chile and C.E.C.S. Casilla 166443, Santiago 9, Chile.

The fast changes in calcium concentration that take place in the triad during E-C coupling may be influenced by metabolites that are produced in this region and that release calcium from the sarcoplasmic reticulum (SR). Using purified transverse tubule (T-T) and heavy SR membranes isolated from frog skeletal muscle, we have found that the enzymes that catalyze the synthesis and degradation of inositol 1,4,5-trisphosphate (IP3), i.e., phosphatidylinositol (PI) kinases, phospholipase C, IP3 phosphatases and PI synthetase, are all present in the T-T membranes.

The SR membranes contain a low affinity IP3 receptor that is part of a calcium release channel present both in native membranes and in purified ryanodine receptors reconstituted in planar bilayers. The effects of IP3 on this channel correlate well with those produced by IP3 on calcium release in permeabilized fibers. Calcium channels, sensitive to caffeine but not to IP3, are also present in heavy SR.

Supported by FONDECYT grants 896, 902 and 972, by MDA and by NIH GM 35981.

W-PM-F1

MUTATIONS AT SITE (M)Y210 IN THE R. SPHAEROIDES RC AFFECT THE INITIAL ELECTRON TRANSFER RATE.

V. Nagarajan[1], W. Parson[1], D. Gaul[2] & C. Schenck[2], [1]Dept. Biochem., Univ. Washington, Seattle, WA 98195 & [2]Dept. Biochem., Colorado S.U., F.C., CO 80523

The unidirectionality of electron transfer from P to BPh_L in RCs and the role of the intervening $BChl_L$ are poorly understood. The crystal structure of R. sphaeroides RCs reveals a Tyr residue ((M)Y210) close to P, $BChl_L$ and BPh_L; the symmetry-related residue on the M-side is Phe. Recent electrostatic energy calculations suggest that the tyrosyl hydroxyl group affects the energetics of transitions to local excited states of $BChl_L$ and the hypothetical state $P^+BChl_L^-$.

To explore the role of (M)Y210 we have performed ps absorption measurements on the site-directed mutants (M)Y210F and (M)Y210I. The decay kinetics of stimulated emission from P* indicate that initial resolved electron transfer in (M)Y210F occurs with a rate constant, k, of $1.1\pm0.1\times10^{11}s^{-1}$. In contrast, k is $2.9\pm0.4\times10^{11}s^{-1}$ in wild-type RCs. (M)Y210I decays in a multiphasic fashion, possibly indicating an increased heterogeneity in the RC; a single exponential fit to the decay at 300K gives a mean value of k of $0.62\times10^{11}s^{-1}$. At 77K, the kinetics in (M)Y210F are unchanged and the mean k in (M)Y210I decreases, in contrast to the increase seen in wild-type. (M)Y210 does indeed play an important role in primary electron transfer. NSF & NIH.

W-PM-F2

ELECTRIC FIELD EFFECTS ON THE SPECTRA AND REACTION DYNAMICS IN WILD-TYPE AND MUTANT REACTION CENTERS.

Steven G. Boxer, Dept. of Chemistry, Stanford University, Stanford, CA 94305

A variety of electric field modulation results on photosynthetic RCs will be discussed. These include: (1) Field modulation of the fluorescence lineshape, the dipole direction in ^1P (co-workers Lockhart, Hammes); (2) Field modulation of electron transfer rates, $^1P\rightarrow P^+H^-$ and $P^+Q^-\rightarrow PQ$ (co-workers Franzen, Goldstein, Lockhart, Holten, Kirmaier); (3) Stark effect on absorption and emission spectra in the *Rb. sphaeroides* heterodimer mutant (co-workers Hammes, Mazzola, Gaul, Schenck); (4) Electric field-induced thermal electron transfer (co-worker Franzen); (5) Spectroscopy and reaction dynamics in D-helix symmetrized *Rb. capsulatus* mutants (co-workers Stocker, Woodbury, Taguchi); (6) Holeburning and field effects in TyrM210→Phe and Ile *Rb. sphaeroides* mutants (co-workers Hammes, Mazzola, Middendorf, Schenck). Supported by NSF Biophysics Program.

W-PM-F3

CHARGE SEPARATION AND RECOMBINATION IN ORIENTED PHOTOSYNTHETIC LANGMUIR-BLODGETT MULTILAYER CAPACITORS FORMED BY VACUUM DEPOSITION.

C.C. Moser and P.L. Dutton, University of Pennsylvania, Philadelphia, PA

The construction of capacitors enclosing Langmuir-Blodgett multilayers of native photosynthetic membranes or purified proteins has been improved by depositing the bulk of the capacitor dielectric by vacuum evaporation of a polymer such as polyethylene, rather than dipping the multilayer in organic solvent polymer solution. Dielectric thickness can be easily measured and controlled by means of a quartz crystal oscillator, permitting us to achieve considerable consistency in sample capacitance and field strength applied the oriented multilayers. The effect of applied field on optically and electronically measured charge separation (including QA to QB electron transfer and perhaps protolytic reactions) and recombination reactions within the reaction center (including recombination from exotic quinones substituted for QA) can be directly compared and provide a means of internal calibration of the applied field strength within the RC.
Supported by PHS grant GM 41048.

W-PM-F4

ELECTROSTATIC CALCULATIONS OF THE RELATIVE MIDPOINTS OF THE COFACTORS OF THE PHOTOSYNTHETIC REACTION CENTER PROTEIN. M.R. Gunner, B. Honig intro. by W.E. Royer. Dept. of Biochem. and Molecular Biophysics, Columbia University, N.Y., N.Y.

The program DelPhi, which solves the poisson equation with a finite difference algorithim, has been used to calculate the relative midpoint potentials of the cofactors and the pKs of the ionizable residues in the reaction center protein (RC) from Rps. viridis. The observed range in midpoints of the 4 hemes in the cytochrome c subunit of 440 meV can be successfully reproduced. The factors that contribute are differences in: the distribution of ionized amino acids (300 meV), solvation energy (70 meV), heme ligands (95 meV) (maximum calculated variation between sites in parenthesis). In addition, the positive charges on the oxidized lower potential hemes increases the midpoints of the higher potential sites by 80-105 meV. The pK dependence of the midpoints and the proton uptake and release on electron transfer within the RC will also be discussed.

W-PM-F5

PROTON BINDING AND ELECTRON TRANSFER IN THE ACCEPTOR QUINONE COMPLEX OF RCs FROM *RB. SPHAEROIDES*

Colin A. Wraight and Peter Maroti
University of Illinois, Urbana, Il 61801, and Institute of Biophysics, Szeged, Hungary.

The primary reactions of photosynthesis produce a series of charge separated states in the reaction center protein complex (RC). In the early stages, solvation of these states plays a varying role in the energetics and kinetics of electron transfer, but it must be substantial for the long lived states, $P^+Q_A^-$ and $P^+Q_B^-$. Although partially screened, the electrostatic disturbance due to the $P^+Q_A^-$ state causes net protonation changes in several amino acid residues of the protein. The kinetics of proton uptake are monophasic but exhibit anomalous pH and temperature dependences which are interpreted in terms of influences of surface potential and rapid conformational changes in the protein.

Transfer of the electron from Q_A^- to Q_B is accompanied by further changes in protonation state of the protein. The kinetics of proton uptake and electron transfer are both complex and cannot be described by a single exponential component in the range pH 7.5 - 9.5. Similar behavior is seen upon transfer of a second electron, to form Q_B^{2-}/Q_BH_2. These results will be discussed in terms of distributed (slow) conformational substates of the protein/quinone structures.

Supported by NSF.

W-PM-F6

PROTON UPTAKE BY RCs FROM Rb. SPHAEROIDES IN WHICH GLU-L212 WAS REPLACED WITH GLN*.

P.H. McPherson, M. Schönfeld†, M.L. Paddock, G. Feher, and M.Y. Okamura, UCSD, La Jolla, CA 92093 and †Hebrew University of Jerusalem, Israel.

Replacement of a putative proton donor to Q_B^{2-}, Glu-L212 , with its non-protonatable analog, Gln, decreased the rate of electron turnover to exogenous quinone ~25 fold (1). This was ascribed to a decrease in the protonation rate, which was assumed to be the bottleneck. To test this model (see Fig.), we have determined at pH 7.5 the rates of proton uptake and electron turnover by the mutant RCs. Proton uptake by $Q_A^-Q_B^{2-}$ was monitored by two methods: i) by pH changes (using dyes), and ii) by electrochromic shifts at 760 nm, which monitor charges (i.e., e^- and H^+) on Q_B. The pH change shows a rapid (< 10 ms) uptake of ~1 proton followed by slow uptake of ~1 proton at a rate $k_{H^+} = 6\pm1\ s^{-1}$. Similarly, the electrochromic shift shows a rapid (< 10 ms) increase in negative charge (formation of $Q_A^-Q_B^{2-}H^+$) followed by a slow decay (formation of $Q_A^-Q_BH_2$) at a rate $k_{H^+} = 6.0\pm0.6\ s^{-1}$, in agreement with the pH changes. The electron turnover rate (to exogenous Q_{10}) was measured by monitoring cytc oxidation. The model predicts a cytc oxidation rate of $2\cdot k_{H^+}$, since 2 cytc are oxidized per cycle. The initial fast (< 10 ms) oxidation of 3 cytc (formation of $Q_A^-Q_B^{2-}$) was followed by a slow turnover at a rate of 12.5 ± 0.4 cytc$\cdot RC^{-1}\cdot s^{-1}$, in agreement with the observed values of $2\cdot k_{H^+}$. These results are consistent with the model and show that Glu-L212 is obligatory for the fast uptake of the second proton.

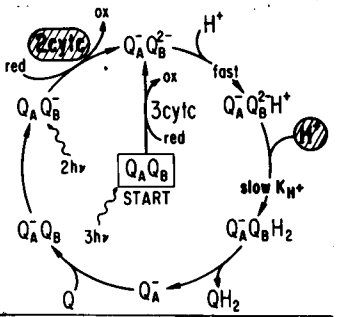

Model of proton uptake and electron turnover in mutant RC.

(1) M.L. Paddock, S.H. Rongey, G. Feher, and M.Y. Okamura (1989), PNAS 86, 6602-6606.

*Supported by NSF and NIH

W-PM-F7

EXOGENOUS Mn^{2+} REDUCES Y_Z^+ IN MANGANESE DEPLETED PHOTOSYSTEM II.

C.W. Hoganson, M. Atamian, Gerald T. Babcock and C.F. Yocum, Department of Chemistry, Michigan State University, East Lansing, MI 48824 and Department of Biology, University of Michigan, Ann Arbor, MI 48901.

Using manganese depleted PSII membranes and flash photolysis with electron spin resonance detection, we examined the reaction between Mn^{2+} or benzidine and Y_Z^+. Kinetics were measured with membranes that did or did not contain the 33 kDa extrinsic polypeptide of PSII, whose presence had no effect with either reductant. The rate of Y_Z^+ reduction by benzidine was a linear function of benzidine concentration. Y_Z^+ reduction rates by Mn^{2+} at pH 6 increased linearly at low $[Mn^{2+}]$ and reached a maximum at $[Mn^{2+}]$ equal to several times the reaction center concentration. The rate of Y_Z^+ reduction at pH 7.5 was biphasic with a fast 400 μs phase that suggests binding of Mn^{2+} near Y_Z^+ at a site that may be one of the native manganese binding sites. (Supported by USDA CRGO.)

W-PM-F8

X-RAY ABSORPTION SPECTROSCOPY OF THE MN SITES IN THE PHOTOSYNTHETIC OXYGEN EVOLVING COMPLEX.

J.E. Penner-Hahn, G.S. Waldo, R.M. Fronko. C.F. Yocum (Intro. by P.L. Dutton). Departments of Chemistry and Biology, University of Michigan, Ann Arbor, MI 48109.

The active site of the photosynthetic oxygen evolving complex (OEC) contains four Mn atoms. We have used x-ray absorption spectroscopy (EXAFS and XANES) to investigate the ligation, nuclearity, and oxidation state of these Mn ions for the OEC in the S_1 state. The average first shell Mn ligation consists of oxygens (and/or nitrogens) at ca. 1.9 and 2.2 Å. In contrast with earlier results, we see no evidence for a significant number of "short" oxygen ligands at ca. 1.75 Å. More distant neighbors include a shell of Mn at 2.7 Å, a Mn-Mn interaction of ca. 3.3 Å, and tentative identification of a shell of Mn and/or Ca at ca. 4.3 Å. Our data, together with published spectroscopic results for the OEC suggest that the Mn are present in a trinuclear cluster and a mononuclear site. Both EXAFS and XANES data indicate that the four different Mn are present in rather different coordination environments. The structural implications of our results, together with recent variable temperature and ligand substitution experiments, will be discussed.

Supported in part by the NIH (GM-38047), the NSF (DCB-15932) and the USDA (CRGO-37130-3546).

W-PM-F9

PHOTOSYSTEM II ELECTRON DONOR AND ACCEPTOR-SIDE FUNCTION PROBED BY SITE-DIRECTED MUTANTS. B.A. Diner, P.J. Nixon, J.G. Metz, M. Rögner, D. Chisholm, DuPont Experimental Station, Wilmington, DE 19880-0173

Site-directed mutants were constructed in PSII reaction center polypeptides D1 and D2 of *Synechocystis* 6803 to probe for residues which participate in electron transfer within the iron-quinone electron-acceptor complex and those which are implicated in ligation of Mn, a redox active cofactor involved in the oxidation of water to molecular oxygen.

Comparision of the primary structure of the reaction center polypeptides of PSII and the photosynthetic bacteria suggests that D1-his252 may be located near the secondary quinone electron acceptor, Q_B. Mutation of this residue to leucine results in a nearly 1000-fold slowing of the rate of electron transfer between quinones Q_A and Q_B, consistent either with an increase in Kd for Q_B binding or a loss of a protonation site coupled to Q_B reduction.

D1-tyr161 is redox active and links the O_2-evolving Mn complex to the primary electron donor, P680. D1-asp170, located near D1-tyr161, was mutated to glu with little effect on O_2-evolution. Replacement of D1-asp170 by ser, however, abolishes O_2 activity but does not prevent photo-oxidation of D1-tyr161 in isolated PS II core preparations. D1-asp170 is, therefore, a potential ligand to Mn.

W-PM-G1

NRL_3D: A SEQUENCE--STRUCTURE DATABASE
K. Namboodiri, N. Pattabiraman, A. Lowrey, B. Gaber, D. G. George*, and Winona C. Barker*, Naval Research Laboratory, Washington, D.C., *National Biomedical Research Foundation, Washington, D.C.
We have developed a new sequence--structure database, NRL_3D, from sequence information extracted from the Brookhaven Protein Data Bank (PDB) and these data have been correlated with those of the Protein Sequence Database (PSD) of the Protein Identification Resource (PIR). The sequence information in PDB is not stored in a format suitable for extensive sequence similarity searches and retrieval. These data have been restructured and the PIR software has been extended to access this information. This software interfaces with standard molecular modeling programs and allows the 3D structure of identified sequences to be displayed directly. This work will form the basis of a direct cross-linkage between PSD and PDB. This work was partially supported by grants from the Office of Naval Research and the U.S. Army Medical Research and Development Command and by grants RR01821 and GM37273 from the NIH.

W-PM-G2

CONFORMATIONS OF MACROMOLECULES IN RESTRICTED SPACES David G. Covell*, Brooke S. Lustig & Robert L. Jernigan, ASCL/PRI/FCRF, Frederick, MD 21701, NCI/DCDB,LMMB, Bethesda, MD 20892.

We present a new method to examine the complete range of folded topologies accessible in the compact state of globular proteins. The procedure is to generate all conformations, with volume exclusion, upon a lattice in a space restricted to the individual protein's known compact conformational space. Using one lattice point per residue we find 10^2 to 10^4 possible compact conformations for the five small globular proteins studied. Subsequently, these conformations are evaluated in terms of residue-specific, pairwise contact energies that favor non-bonded, hydrophobic interactions. Native structures for the five proteins are always found within the best 2% of all conformers generated. This novel method is simple and general and can be used to determine most favorable overall packing arrangements for the folding of specific amino acid sequences within a restricted space.

W-PM-G3

CONFORMATIONAL STUDIES OF NISIN AND ITS FRAGMENTS BY NMR AND COMPUTER SIMULATIONS

D. E. Palmer and M. Goodman
(U.C. San Diego, La Jolla, CA 92093)

We propose structures for the peptide antibiotic nisin, and active fragments. Nisin contains five constrained rings with some unusual constituents: α,β-unsaturated amino acids and lanthionine (monosulfide) bridges. These same features appear in other naturally-occurring antibiotics such as epidermin and subtillin; possibly playing a role in antibiotic activity. Such constrained structures exhibit strong conformational preferences, which facilitate both our spectroscopy and computer simulations. NMR spectroscopy has been carried out on the entire 34-amino acid molecule, nisin 1-32, as well as fragments containing each of the rings. Temperature coefficients and nuclear Overhauser enhancements (NOE's) were measured in DMSO-d_6 for each compound. High temp. (750K-1000K) molecular dynamics, followed by energy minimizations ±NOE yeilded low energy conformations for each ring. From these, molecular dynamics proceeded at 300K. Simulated properties agreed well with NMR. The lowest energy conformations were assembled to determine low energy conformations of the larger fragments as well as whole nisin. The computer simulations were carried out using DISCOVER. Force constants and structural parameters for the α,β-unsaturated amino acids were determined through X-ray diffraction analysis, IR spectroscopy and *ab initio* calculations.

W-PM-G4

SOLVATION ENERGY OF PROTEIN INTERFACES

S. Watowich, T. Herron and R. Josephs
University of Chicago, Chicago, Illinois

Solvent effects play a major role in stabilizing protein conformations, interactions and assemblies. Following the approach of Eisenberg and McLachlan [Nature 319, 199 (1986)] we present a method for calculating the relative energy of solvent-protein interactions. Individual residue contributions are normalizied relative to glycine such that differences in solvation energies are comparable to differences in surface areas for protein's in the same asymmetric unit.

Solvation free energies per unit surface area (Δg) are calculated for oligomeric proteins. Interfaces with large positive Δg are classified as highly hydrophobic; interfaces with Δg similar to those assigned to the solvent-accessible surface of the protein are classified as weakly hydrophobic. The interface between $\alpha 1$ and $\beta 1$ subunits of deoxyhemoglobin (dHb) is highly hydrophobic while the interface between $\alpha 1 \beta 1$ and $\alpha 2 \beta 2$ subunits of dHb is only weakly hydrophobic. For FAB-lysozyme complexes the interface has large positive Δg values. This contrasts to the negative Δg value found for the surface of uncomplexed lysozyme, implying that hydrophobic effects may play a role in FAB-lysozyme association. Supported by NIH grants HL02277 (SW), HL22654 and HL30121 (RJ).

W-PM-G5

INVESTIGATION OF THE SOLVATION ENERGIES OF ALPHA HELICES

Anthony Nicholls and Barry Honig, Dept. of Biochemistry and Biophysics

The Poisson-Boltzmann equation allows for an accurate evaluation of electrostatic energies of macro-molecules in aqueous, ionic enviroments. Using the DelPhi electrostatics program to solve this equation, we have looked at the energetics of the desolvation of alpha helices, i.e. removal from exposure to solvent (details in Gilson and Honig, PNAS, Vol.86, pp.1524). This may occur, for example, upon tertiary folding of a protein, or insertion into a membrane. Calculations for the latter brings to light interesting properties, such as a 'bulk' desolvation penalty, as well as the expected end effects due to the helix dipole. The consequences for insertion of proteins into membranes are examined.

W-PM-G6

EFFECT OF AMINO ACID REPLACEMENTS ON A PEPTIDE HELIX/COIL TRANSITION.

Gene Merutka and Earle Stellwagen. Department of Biochemistry, University of Iowa, Iowa City, IA 52242.

The peptide acetylYEAAAKEAAAKEAAAKAamide exhibits a thermal dependent helix/coil transition in aqueous solution at neutral pH which was observed by far ultraviolet circular dichroic measurements. Analogs of this peptide were synthesized by the T-bag method and purified by RP-HPLC. The fidelity of each synthesis was established by amino acid analysis and by FAB-mass spectroscopy. Each thermal transitions at 222 nm was fit with a sigmoidal curve having a span of 33,500 deg cm^2dmol^{-1}. Replacements at positions 4, 9 or 14 have an equal effect on the thermal dependence, while multiple replacements at these positions have an additive effect. Replacement of ala 9 with the other 19 amino acids changes the thermal dependence of the helix/coil transition largely as predicted by residue helix propensity values obtained from analysis of crystallographic models of proteins. (Supported by NIH grant HE-14388).

W-PM-G7

THERMODYNAMIC FEATURES COMMON TO PROTEIN UNFOLDING AND DISSOLUTION OF HYDROPHOBIC COMPOUNDS IN WATER

Kenneth P. Murphy*, Stanley J. Gill*, and Peter L. Privalov+

*Department of Chemistry and Biochemistry
University of Colorado
Boulder, Colorado 80309-0215

+Institute of Protein Research
Academy of Sciences of the USSR
Moscow Region, USSR

Protein unfolding and dissolution of hydrophobic compounds (including solids, liquids, and gases) in water show linear correlation of entropy change versus heat capacity change. The same slope is found for various classes of compounds, whereas the intercept depends on the particular class. The feature common to these processes is exposure of hydrophobic groups to water. These observations enable assignment of the heat capacity change to hydrophobic solvation and lead to the description of protein stability in terms of a hydrophobic and a nonhydrophobic contribution. A general representation of protein stability is given by the heat capacity change and the temperature. (Supported by NSF grant CHE-8611408)

W-PM-G8

KINETIC EVIDENCE OF THE COMPLEXITY OF THE UNFOLDED STATE OF STAPH. NUCLEASE.

Robell H.M. Chen & Tian Yow Tsong. Dept of Biochem, Univ of Minnesota, St. Paul, MN 55108.

Current interest in the folding/unfolding of WT and mutant nucleases, prompted us to re-investigate kinetics of the pH induced transitions of the WT. Kinetics in the time range 2 ms to 300 s were examined with a stopped-flow (Hi-Tech), monitoring fluorescence changes of Trp 140. At 25°C, ionic strength 0.125, both acidic (mid point pH 3.9) and alkaline (mid point pH 10.4) transitions showed 3 kinetic phases in folding and one kinetic phase in unfolding, indicating that the folding involves 3 kinetic steps whereas the unfolding is a one step reaction. The simplest mechanism is, $D_3 - D_2 - D_1 - N$. The acidic unfolding was catalyzed by H^+ and the alkaline unfolding was catalyzed by OH^-. All reactions of the folding were independent of pH from 6 to 8. In the folding from acid (pH 3.1 to 7.0), the activation energies (E_a) were 6.0, 5.6 and 13.4 kcal for the 155 ms, the 860 ms, and the 30.0 s reactions, respectively. E_a was 28.7 kcal for the unfolding from pH 7.0 to 3.1. These results contrast the early reports that the fast reactions in folding exhibit no E_a and are, thus, assigned the nucleation events of the protein folding. [Supported by NIH Grant GM 37304]

W-PM-G9

Quaternary Structure and Interaction Energies of Single Site Mutants of *E. Coli* Aspartate Transcarbamylase. D.S. Burz and N.M. Allewell, Wesleyan University, Middletown, CT 06457; J.M. Sturtevant, Yale University, New Haven, CT 06520.

Effects of single site mutations on the Stokes' radius and subunit interaction energies were evaluated by analytical gel chromatography and differential scanning calorimetry. Partition coefficients of proteins with mutations at the interface between catalytic subunits are consistent with conclusions drawn from activity measurements, that they result in shifts in the T<-->R equilibrium. These mutations alter c:r interactions as indicated by changes in the Tm and ΔH of the thermal transition of the regulatory subunit in the holoenzyme. Mutations between chains in the catalytic subunit give rise to Stokes' radii smaller than that of the T state and a single thermal transition at the Tm of regulatory subunits in the holoenzyme. Supported by NIH grants DK-17335 (to NMA) and GM-04725 (to JMS) and NSF grant DMB-8421173 (to JMS).

W-PM-G10

POINT CHARGE INTERACTIONS IN THE ELECTROSTATICS OF ENZYME/SUBSTRATE ENCOUNTER: A KINETIC ANALYSIS USING BROWNIAN DYNAMICS OF CU/ZN SUPEROXIDE DISMUTASE MODELS. Jacqueline J. Sines*, Stuart A. Allison, Dept. of Chem., Georgia State Univ., Atlanta, GA 30303. J. Andrew McCammon, *Dept. of Chem., Univ. of Houston, Houston, TX 77204-5641. (*Current address) Brownian Dynamics simulations using linearized Poisson-Boltzmann potentials were used to study electrostatic steering of a substrate ion into an enzyme's active site. Single and multiple modifications in the point charge distribution of the enzyme define models with altered electrostatic potential fields. The model system employed is the diffusion of the superoxide radical anion to the active site of bovine erythrocyte Cu/Zn superoxide dismutase (SOD). Comparisons of SOD models having multiple point charge modifications with models having the component single modifications show that, in general, the electrostatic effects of these alterations on reaction rates are multiplicative. Exceptions are observed when component charges are located within the active site channel. These results may be generalized to predict the electrostatic effects of multiple amino acid substitutions when the effects of single substitutions are known.